Tectonophysics 510 (2011) 253–268

Contents lists available at SciVerse ScienceDirect

Tectonophysics

journal homepage: www.elsevier.com/locate/tecto

The mechanical paradox of low-angle normal faults: Current understanding and open questions

Cristiano Collettini

Dipartimento di Scienze della Terra Università degli Studi di Perugia, Italy
Istituto Nazionale di Geofisica e Vulcanologia, Roma, Italy

ARTICLE INFO

Article history:
Received 5 March 2011
Received in revised form 18 July 2011
Accepted 24 July 2011
Available online 9 August 2011

Keywords:
Low-angle normal faults
Friction
Fault mechanics
Seismicity

ABSTRACT

Low-angle normal faults, LANF, (dip<30°) have been proposed as key-structures for accommodating crustal extension. In contrast, frictional fault reactivation theory predicts that slip on LANF is extremely unlikely: this prediction is consistent with the absence of moderate-to-large earthquakes on normal faults dipping less than 30°.

In order to discuss this discrepancy I will analyse and integrate: 1) geological data from 9 LANF, 2) the dip-range of earthquake-ruptures in extensional environments, and 3) frictional fault mechanics.

LANF fault zone structure is represented by two end members: a) a thick mylonitic shear zone superposed by cataclastic processes and some localization; 2) a discrete fault core separating hangingwall and footwall blocks affected by brittle processes. LANF act as preferential channels for fluid flow and in some cases they promoted fluid overpressure. Fluid–rock interactions along some detachments favour the development of phyllosilicates that in general are characterised by low frictional strength, $\mu<0.4$, and inherently stable, velocity-strengthening frictional behaviour. The low friction coefficient of the phyllosilicates can explain movements on LANF and the velocity strengthening behaviour of the phyllosilicates implies fault creep and therefore can be used to explain the absence of moderate-to-large earthquakes on LANF in seismological records.

However in my view, the integration of the three datasets does not provide a simple mechanical solution for the LANF paradox since it leaves two important open questions. First a widespread development of phyllosilicates does not seem to be a common feature for most of the exhumed LANF that on the contrary show the typical fault rocks of the brittle and seismogenic crust. Second, although some brittle detachments reactivated pre-existing ductile shear zones, others formed as gently dipping structures within a brittle crust characterised by a vertical σ_1: a well constrained mechanical explanation for this second class of structures is lacking.

Contents

E-mail address: colle@unipg.it.

0040-1951/$ – see front matter © 2011 Elsevier B.V. All rights reserved.
doi:10.1016/j.tecto.2011.07.015

1. Introduction

Over the past 40 years, very low dipping (0–30°) normal faults, low-angle normal faults (LANF) or extensional detachments, have been extensively mapped in areas of continental extension (Fig. 1). These structures have been firstly recognised in the Basin and Range province, US, (Anderson, 1971; Longwell, 1945; Wernicke, 1981) and then documented in most of the tectonic settings affected by crustal extension.

Geological evidence suggests that such structures accommodated a significant amount of crustal extension (also within the brittle crust) at dips similar to their present attitude and within a regional stress field characterised by vertical σ_1 trajectories (e.g. Fig. 1, Collettini and Holdsworth, 2004; Hayman et al., 2003; John and Foster, 1993; Jolivet et al., 2010; Lister and Davis, 1989). Associated fault rocks (gouge, breccia, cataclasite, and rare pseudotachylyte) suggest that these structures were predominantly of brittle-frictional character and were formed in the upper seismogenic crust at low dips (cf. paragraph 2 and references therein). In some large displacement detachments, the gently dipping attitude is favoured by isostatic adjustments (Spencer, 1984; Wernicke and Axen, 1988). In contrast, other geological studies suggested that detachments are not relevant for accommodating crustal extension because: a) they initially formed at steep angles but then progressively rotated, whilst inactive, down to lower dips through domino rotation of younger sets of steeply dipping normal faults (Proffett, 1977); and b) they are interpreted as rootless gravity slides (e.g. Walker et al., 2007).

Seismological evidence suggests that moderate-to-large extensional earthquakes nucleate on moderate-to-steeply dipping structures, peaking at 45° (Collettini and Sibson, 2001; Jackson and White, 1989; Molnar and Chen, 1982; Thatcher and Hill, 1991). Possible seismic activity on low-angle normal faults has been proposed in Papua New Guinea, Gulf of Corinth (Greece) and Apennines (cf. paragraph 3).

Anderson–Byerlee frictional fault reactivation theory, i.e. an extending crust characterised by vertical trajectories of σ_1 and normal faults possessing friction in the range of 0.6–0.85 (Byerlee, 1978), predicts that it is easier to form a new optimally oriented fault (dip about 60°) instead of reactivating an existing one dipping less than 30° (Collettini and Sibson, 2001; Sibson, 1985).

Several manuscripts have provided reviews on different aspects of the extensional detachment enigma focussing on their origin (Lister and Davis, 1989), their possible seismogenic role (Wernicke, 1995) and their mechanics (Axen, 2004; Abers, 2009). In this manuscript I will review: a) fault geometry and fault rocks for 9 LANF that were active within the brittle crust (paragraph 2), b) the dip distribution for earthquake-ruptures in extensional environments (paragraph 3), and c) the Coulomb criterion and frictional fault reactivation theory of brittle faults (paragraph 4). Data presented in these three paragraphs will be integrated in a final discussion on fault structure, fluid flow, fault rocks, mechanical properties and possible seismic behaviour of low-angle normal faults (Fig. 1).

1.1. Adopted terminology

A widely cited conceptual fault zone model suggests that seismically active, upper crustal *brittle* faults pass down, across a predominantly thermally activated transition at 10–15 km depth, into *ductile* shear zones in which deformation occurs by aseismic viscous creep (Imber et al., 2001; Schmidt and Handy, 1991; Scholz, 2002; Sibson, 1977). *Brittle faults* are mainly affected by discrete and localised deformation within rocks displaying elasto-frictional behaviour (e.g. Sibson, 1977). *Ductile shear zones* are mainly characterised by viscous creep processes (Schmidt and Handy, 1991) such as crystal plasticity (Drury and Urai, 1990; Hirth and Tullis, 1992) and grain-size sensitive diffusion creep (Rutter, 1983; Schmidt and Handy, 1991). The *Brittle–ductile* or frictional–viscous transition is the zone at which elastic-frictional behaviour switches into viscous creep.

Random-fabric fault rocks formed by elasto-frictional behaviour are (Sibson, 1977): *gouge, breccia, cataclasite-series and pseudotachylyte*. Foliated fault rocks formed by viscous processes are *mylonites*. For

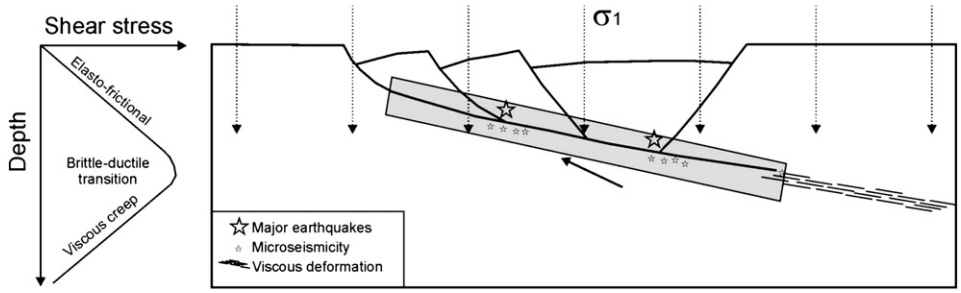

Fig. 1. Schematic representation of a crustal scale low-angle normal fault. In this review: a) field data from detachments exhumed from the brittle crust (fault rocks, mineralogy and minor structures used to infer the orientation of σ_1); b) seismological data (earthquake-rupture dip) for extensional environments; and c) frictional fault reactivation theory, will be analysed and integrated in order to discuss about the mechanics of low angle normal faults within the brittle crust (grey area).

the other foliated rocks not associated to crystal plastic processes I will specify where possible the deformation mechanism, e.g. *SCC' fabric* formed by dissolution precipitation processes (e.g. Bos and Spiers, 2001) or *YPR fabric* formed by cataclastic processes (e.g. Chester et al., 1985; Cowan et al., 2003).

2. Detachment faults: fault zone structure and fault rocks

In the following paragraph I will summarise field studies of detachment faults from the Basin and Range, Greece, Alps, Turkey and Apennines (Table 1). In particular I will focus on fault geometry (i.e. dip of the detachment and orientation of the regional stress field during the fault activity) and fault rocks, with particular attention to those structures formed within the brittle crust. For further details of the geology of each case-study analysed in this review I suggest the readers to consult the cited literature.

2.1. The Whipple Mountains detachment, California

The Whipple Mountains detachment of south eastern California has a total displacement of at least 40 km accumulated during lower Miocene (Davis, 1986a, 1986b; Davis et al., 1986a; Lister and Davis, 1989). The shallower part of the fault zone formed at less than 2–3 km depth since it truncates sub-horizontal Miocene strata and this part of the stratigraphic section is less than 2–3 km thick. The intersection angle (cut-off) between the fault and the Miocene strata does not exceed 10–15° implying that the fault cannot represent a formerly steep normal fault which has been rotated into shallow attitude by ongoing extension. The Whipple low-angle normal fault formed with a dip of 10–15° and analysis of fractures distribution constrain a steep to vertical σ_1 in the upper plate (Axen and Selverstone, 1994; Lister and Davis, 1989; Reynolds and Lister, 1987). The present Whipple detachment fault system is interpreted as an amalgamation of several generations of gently dipping normal faults and shear zones formed at

Table 1
Dip, fault structure and fault rocks from extensional detachments exposed at the Earth's surface. The description of the fault rocks is focussed on brittle structures.

LANF	Mean dip	Fault structures	References
Whipple	10–15°	Lower Miocene activity in a stress field with vertical regional σ_1. Mylonites superposed by fault breccia: the development of a chlorite-rich breccia suggests build-ups of fluid overpressures along the detachment at the brittle–ductile transition. At shallower crustal levels a planar surface caps quartz-rich ultracataclasites. Rare pseudotachylytes.	Davis et al., 1986; Lister and Davis, 1989; Reynolds and Lister, 1987.
South Mountains	10–20°	Lower Miocene activity in a stress field with vertical regional σ_1. SC mylonites overprinted by cataclasites. Cataclasites are composed of quartz, feldspar and different amount of biotite. Pseudotachylytes formed along C surfaces at the brittle-ductile transition.	Davis et al., 1986; Goodwin, 1999.
Chemehuevi–Sacramento	<20°	The fault formed in the Lower Miocene as a low angle structure and it was active within the brittle crust in a stress field with vertical regional σ_1. Minor zones of deformation represented by 0.001–1 m thick, quartz-feldspathic, mylonites are overprinted by hydrothermally altered cataclasites rich in chlorite–epidote ± calcite. Rare pseudotachylyte veins a few millimetres thick and up to 0.5 m long. Recent planar surface made of a chlorite-rich cataclasite with a thin layer of illite and smectite rich fault gouge.	John, 1987; John and Cheadle, 2010.
Black Mountains	19–36°	Pliocene–Quaternary activity in a regional stress field with a vertical regional σ_1. Fault zone made of a foliated breccia and fault gouge. A principal slip plane is located at the top of the detachment. The footwall shows small displacement faults, fractures, veins and areas rich in chlorite-epidote. The dominant constituents of matrix (10–40%) are phyllosilicates (illite, chlorite, illite–smectite and chlorite–saponite).	Cowan et al., 2003; Hayman et al., 2003; Hayman, 2006.
Tinos	20°	Slip at 30–15 Ma in a regional stress field with a vertical regional σ_1. Mylonites overprinted by cataclasites. Cataclasites formed at the expenses of serpentinite and micaschists: dense veining and the development of syntectonic minerals like talc suggest intense fluid rock interaction.	Katzir et al., 1996; Famin et al., 2004; Jolivet et al., 2010.
Mykonos	12–18°	Slip at 14–9 Ma in a regional stress field with a vertical regional σ_1. Mylonites overprinted by brittle fault rocks. Cataclasites (quartz-feldspar in a phyllosilicate-rich matrix) or brecciated metabasites in the footwall block passing to fault gouge into the fault zone. The fault gouge consists of sub-rounded quartz-clasts within a fine-grained matrix that represents up to 75% of the fault rock. The matrix is made of Illite, dickite and goethite.	Lecomte et al., 2010; Lecomte, 2010.
Err Nappe	<20°	Formed along a Jurassic continental rifted margin. Fault core made of a continuous layer of black gouge, with thickness ranging from a few centimetres to some metres. In the footwall the granitic host rock is affected by brittle fracturing associated with a complex vein system. Towards the fault core the matrix to clast ratio increases leading to a matrix supported SC fabric. The amount of phyllosilicates (chlorite, Illite) increases to more than 60% in the black gouge	Manatschal, 1999.
Alaşehir	10–30°	Neogene high angle normal fault rotated the fault to shallower dips. Mylonites overprinted by brittle fault rocks. The brittle fault rocks (rich in quartz, feldspar and biotite) consist of breccia, cataclasite, foliated cataclasite and pseudotachylytes. Cataclasites show fractures and numerous veins rich in calcite and fe-oxides. The percentage of clasts to matrix ratio ranges from 75 to 5%: the matrix consists of varying amounts of quartz, chlorite, Fe-oxides, sericite, epidote and carbonate. The top of the cataclasite consists of a discrete shear zone.	(Isık et al., 2003).
Zuccale	<20°	The fault formed and slipped (13–4 Ma) as a low-angle normal fault in a regional stress field with a vertical regional σ_1. In the early stages of the activity cataclasis facilitated the influx of chemically active fluids that promoted the syn-tectonic growth of talc, chlorite and smectite. In the later stages, foliated cataclasites formed by rolling and sliding of grains (quartz and dolomite) past one another along clay-lined (illite) grain boundaries. The foliated cataclasites are cut by thin (<1 cm) and striated principal slip surfaces. Veins, rich in calcite and dolomite, suggest local build-ups in fluid pressure.	Collettini and Holdsworth, 2004; Collettini et al., 2006; Smith et al., 2007; Collettini et al., 2009a; Smith et al., 2011b.

different crustal depths (Lister and Davis, 1989). The fault rocks preserved along the shear zones allow to constrain the deformation processes operating at different crustal depths during exhumation (Lister and Davis, 1989). The lower plate is generally characterised by both a non-mylonitic basement and a 0.1–4 km thick mylonitic gneiss that is locally overprinted by narrow (0.1–10 cm) mylonitic shear zones (Davis, 1988; Lister and Davis, 1989). These fault rocks formed in the ductile field by crystal plastic processes. During fault exhumation mylonitic fault rocks are replaced by a chlorite-rich breccia: the development of the chlorite rich breccia is favoured by fluid overpressures trapped along the detachment near the brittle–ductile transition (Lister and Davis, 1989). The shallower part of the fault zone is represented by a planar surface that caps quartz-rich ultracataclasites and in some outcrops some pseudotachylytes have been documented. In the exposed outcrops only small areas of contiguous pseudotachylytes have been reported (Lister and Davis, 1989), and possible explanations for the limited exposures can be related to alteration with time and exhumation, or small earthquakes associated to the detachment (Lister and Davis, 1989).

2.2. The South Mountains detachment, Arizona

The South Mountains detachment, Arizona, was active as a low-angle extensional structure, with a dip of about 10°, as highlighted by palaeomagnetic data (Livaccari et al., 1993). Sub-vertical extension fractures, oriented perpendicular to the transport direction and formed during the earliest phase of brittle deformation, constrain a vertical regional σ_1 during the fault activity (Reynolds, 1985). Deformation along the shear zone occurred over a range of temperatures as lower Miocene plutonic intrusions in the footwall block were broadly contemporaneous with fault activity (Goodwin, 1999; Reynolds et al., 1986). Gently dipping (10–20°) mylonites, formed below or near the brittle ductile transition, were progressively uplifted above the brittle–ductile transition and were overprinted by brittle structures (Reynolds, 1985). The S–C mylonites are made of feldspar, quartz and biotite and all minerals are elongated parallel to the S-surfaces (Goodwin, 1999). During the later stages of extension cataclasites and pseudotachylytes formed. In particular, both cataclasites and pseudotachylytes are typically subparallel to C-surfaces of the mylonite. Cataclasites are composed of quartz, feldspar and different percent of biotite whereas pseudotachylytes are always associated to biotite (Goodwin, 1999). Most pseudotachylyte veins show varying degrees of mylonitic overprinting. The formation of pseudotachylytes in the foliated granitoid is related to seismic failure along gently dipping C-surfaces: again it is worth noting that lateral continuity in pseudotachylyte veins is limited (Goodwin, 1999).

2.3. The Chemehuevi Mountains detachment, California and Arizona

The Chemehuevi-Sacramento detachment fault, displacement>18 km and dip<20° (Howard and John, 1987), represents a continental detachment within the brittle crust (<10 km) and it deforms footwall rocks comprising quartzo-feldspathic basement and/or syntectonic plutonic rocks with little pre-existing deformation fabric (John and Cheadle, 2010). The hangingwall block is affected by numerous high-angle normal faults that rotated to more gentle dips through time and do not cut the detachment (Howard and John, 1987). Structural and thermochronologic data suggest that low-angle normal faulting initiated (24–22 Ma) and was active within the seismogenic regime at moderate to low angles (John and Foster, 1993). In addition, coeval steep normal faulting with detachment development implies a steep orientation of the regional σ_1 (John and Foster, 1993). In the footwall block of the detachment fault rocks exhumed from different crustal depths are located in a deformation zone with thickness ranging from 1 to 100 m. The structurally deepest fault rocks develop along minor zones of deformation represented by 0.001–1 m thick mylonites (John, 1987; John and Foster, 1993). These quartz-feldspathic fault rocks are overprinted (generally in the footwall beneath the detachment) by hydrothermally altered cataclasites rich in chlorite–epidote ± calcite (John and Cheadle, 2010). Rare veins of pseudotachylytes a few millimetres thick and up to 0.5 m long are locally recognised. The most recent slip surface is a planar zone which comprises a chlorite-rich cataclasite with a thin layer of illite and smectite rich fault gouge (John and Cheadle, 2010).

2.4. The Black Mountains detachments

The Black Mountains detachments define the upper surface of the Mormon Point, Copper Canyon and Badwater "turtlebacks" (Wright et al., 1974). The rocks exposed in the footwall of most detachments are late Proterozoic carbonate and siliceous gneisses, which are the early Proterozoic quartzo-feldspathic basement, and late Miocene plutonic rocks. In the hangingwall blocks Quaternary–Pliocene sedimentary rocks are exposed (e.g. Drewes, 1963). Steeply dipping and listric normal faults in the hangingwall block sole into and do not cut the low-angle (dip 19°–36°) detachment, implying slip on the detachment in a regional stress field with a vertical σ_1 (Hayman et al., 2003). The deformation along the detachment is asymmetrically distributed, increasing upward from the footwall into a foliated breccia and fault gouge (Fig. 2 and Cowan et al., 2003). Fault rocks testify deformation processes occurring from ≥3 km to near-surface conditions (Hayman, 2006). A principal slip plane is located at the top of the detachment whereas other Y, P and R structures cut the gouge and the foliated breccia (Fig. 2b and c; Cowan et al., 2003). The contact between the foliated breccia and footwall is generally gradational and small displacement faults, fractures, veins (rich in siderite, hematite or tourmaline) and areas rich in chlorite–epidote extend from the footwall into the shear zone (Fig. 2 and Hayman, 2006). The foliated breccia is characterised by a cataclastic texture in a fine grained matrix with granular domains between larger clasts. The fault gouge (Fig. 2c) is represented by grains, with abraded grain boundaries, that rotate and translate within a fine-grained matrix. Clasts are made of quartz, feldspar, carbonates or have the more heterogeneous mineralogy of mica-rich schists. The dominant constituents of matrix, that represent 10–40% of the fault rocks, are phyllosilicates: illite, chlorite, illite–smectite and chlorite–saponite (Hayman, 2006).

2.5. The North Cycladic detachment system

The North Cycladic detachment system is composed of a series of detachments cropping out in the islands of Andros, Tinos and Mykonos, separating the Cycladic Blueschists in the footwall from the Upper Cycladic Nappe in the hangingwall (Jolivet et al., 2010). The ductile (crystal-plastic processes) detachments generally reactivated former thrusts with a low-dip, and they kept the same attitude during their exhumation and reactivation within the brittle field (Jolivet et al., 2010). Tinos and Mykonos detachments will be analysed in this review.

Tinos detachment (30–15 Ma, Jolivet et al., 2010) is characterised by an evolution from ductile to brittle as the footwall crossed the brittle–ductile transition during exhumation. The hangingwall block of Tinos detachment is made of ophiolitic material, serpentinite, gabbros and minor basalts (Katzir et al., 1996). The footwall block is represented by mylonitic micaschists and marbles (Jolivet et al., 2010). In the footwall block the deformation is accommodated by numerous shear bands that become more intense approaching the detachment. In the footwall block, vertical syntectonic veins and minor high-angle normal faults constrain a vertical σ_1 during the activity of the fault. The detachment (mean dip 20°) is characterised by cataclasites formed at the expenses of serpentinite and micaschists: dense veining and the development of syntectonic minerals

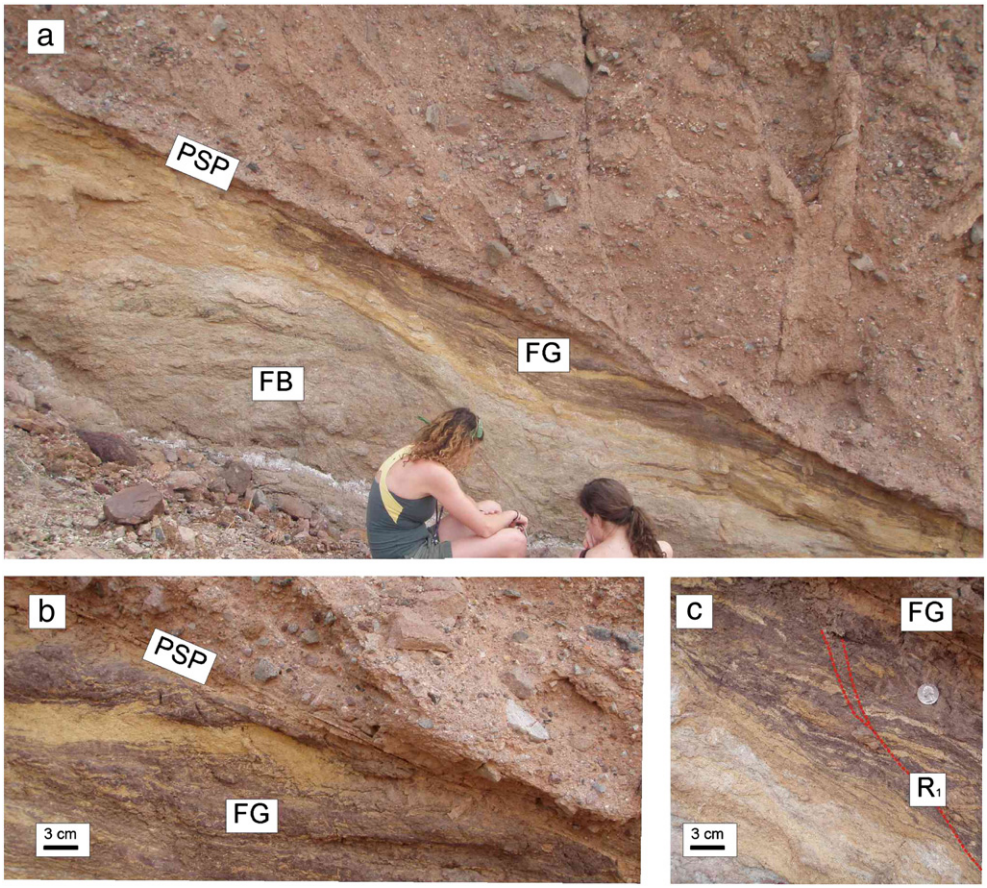

Fig. 2. The Black Mountains detachments. a) Outcrop photograph of the Badwater turtle back fault where a principal slip plane, PSP, separates hangingwall Quaternary fanglomerates from fault rocks consisting of foliated fault gouge, FG, and foliated fault breccia, FB. The fault rocks were derived primarily from the footwall consisting of Proterozoic quartzo-feldspathic gneiss and marble. b) Close-up view of the PSP–FG contact and c) foliated fault gouge with R_1 Riedel shear planes. Details of the fault rocks are presented in Cowan et al. (2003) and Hayman (2006). Photographs taken by DS Cowan.

like talc suggest intense fluid rock interaction (Famin et al., 2004; Jolivet et al., 2010).

The Mykonos detachment system developed during and after a granite intrusion. The internal structure of the fault system is represented by two shallow dipping detachments (dip range 12–18°): the Livada detachment (14–10 Ma Jolivet et al., 2010) and the Mykonos detachment (14–9 Ma Jolivet et al., 2010). The Livada detachment superposes metabasites above a foliated granite: the shear zone consists of ultramylonitic and mylonitic shear bands (Lecomte et al., 2010). Locally the metabasites–granite contact is reworked by brittle low-angle normal faults either localised at the top of the ultramylonite or cutting through it. The Mykonos detachment separates a hangingwall block consisting of conglomerates and sandstones from a footwall block represented by metabasites or granites (Fig. 3 and Lecomte et al., 2010). The high-angle normal faults that sole into the detachment, the vertical barite and Fe-hydroxide veins (some of them cut by the detachment) and the relationship between the dip of the sedimentary rocks and the detachment imply movement on the normal fault at low dips and in a stress field with vertical σ_1 (Lecomte et al., 2010). When the detachment superposes brecciated sedimentary rocks on the top of the granite the fault zone is made of a cataclastically deformed granite and thin zones (about 10 cm) of fault gouge and ultracataclasites (Fig. 3c, Lecomte et al., 2010). The cataclasite consists of fractured clasts of quartz and feldspar in a phyllosilicate rich matrix made of illite and kaolinite (Lecomte, 2010); the fault gouge shows the same mineral phases but here the phyllosilicates increases up to 30% of the fault rocks (Lecomte, 2010). When the detachment superposes sedimentary rocks on top of metabasites the fault zone is made of (bottom to top): brecciated metabasites (4–5 m in thickness), 50 cm-tick powdery gouge, passing upward to foliated gouge (Fig. 3b, Lecomte et al., 2010). The fault gouge consists of sub-rounded quartz-clasts within a fine-grained matrix that represents up to 75% of the fault rock: quartz, Illite, kaolinite and goethite are present within the matrix (Lecomte, 2010).

2.6. Detachment in the Err Nappe, Eastern Alps

A regional detachment, displacement>11 km, developed in a brittle quartzo-feldspathic upper crust is well exposed in the Err Nappe in eastern Switzerland (Manatschal, 1999). The fault formed along a Jurassic, continental rifted margin. The gently dipping attitude of the structure is documented by the low-angle between bedding in the syn-rift sediments onlapping the detachment, and the detachment fault plane (Manatschal and Nievergelt, 1997). The fault core of the detachment is made of an almost continuous layer of black gouge, with variable thickness ranging from a few centimetres to some metres. At the microscale the fault fabric is represented by a foliated fault rock (S–C fabric formed by diffusion mass transfer processes) with detachment-parallel shear zones that are enriched in phyllosilicates (illite and chlorite). The occurrence of graphite may cause the black colour of the gouge (Manatschal, 1999). In the footwall block of the detachment the granitic host rock is affected by brittle fracturing associated with a complex vein system. Towards the main detachment: 1) the matrix to clast ratio increases leading to a matrix supported foliated fabric; and 2) the veins become interconnected and deformation starts to develop along detachment parallel veins. The relative amount of feldspar in the fractured footwall block is

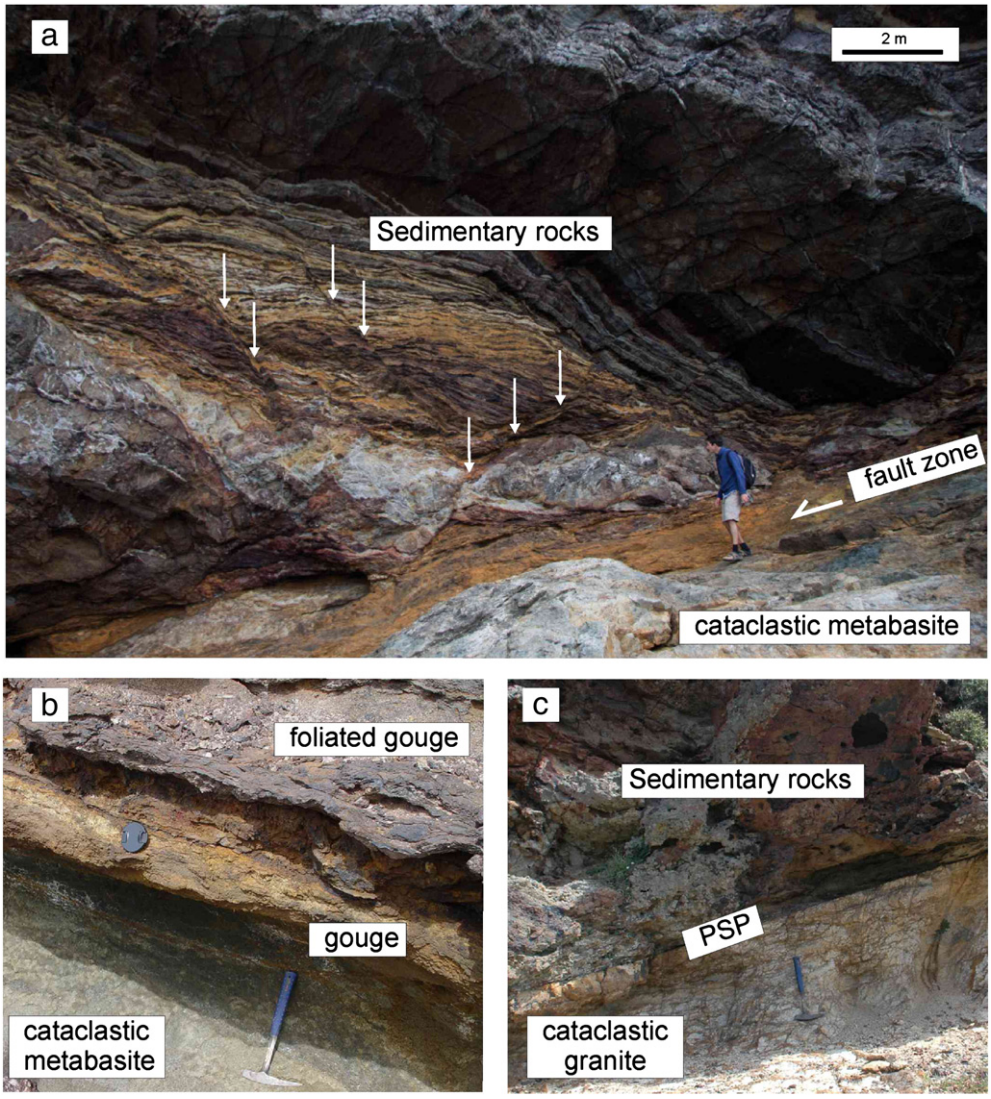

Fig. 3. a) Outcrop photograph of the Mykonos detachment, Greece (details in Lecomte, 2010; Lecomte et al., 2010). The high angle normal faults (highlighted by the white arrows) that sole into the basal low-angle normal fault constrain movements along the detachment in a stress field with vertical σ_1. b) and c) details of the fault rocks and principal slip plane, PSP. Photographs taken by E. Lecomte.

between 40 and 70% whereas in the fault core it is below 10%. In the fractured footwall block the amount of phyllosilicates is between 10 and 40% and it increases to more than 60% in the black gouge (Manatschal, 1999). Deformation in the hangingwall block is limited to small displacement high- and low-angle normal faults.

2.7. The Alaşehir detachment fault, Western Turkey

In the Menderes massif, western Turkey, extensional deformation resulted in the formation of detachment faults and high angle normal faults (e.g. Gessner et al., 2001; Isık et al., 2003; Ring et al., 1999). The Alaşehir detachment is a regional scale low-angle normal fault which separates Neogene sedimentary rocks of the Alaşehir graben in its hangingwall, from metamorphic rocks and granodioritic intrusions in its footwall (Isık et al., 2003). The shear zone has a dip of about 10–30° and it is characterised by a width ranging from 0.5 to 3.5 km. In the hangingwall block high angle faults sole into the detachment (Isık et al., 2003). During the activity of the hangingwall faults the detachment rotated to shallower dips (Gessner et al., 2001) and was still active (Isık et al., 2003) presumably in a stress field with vertical σ_1. The Alaşehir shear zone contains mylonites, formed in the early stages of deformation, that are overprinted by brittle fault rocks. The mylonitic shear zone is composed of protomylonites, mylonites and thin laterally discontinuous ultramylonites: alterations of some biotites to chlorite is common (Isık et al., 2003). The mylonitic fault rocks grade upward into a brittle shear zone with a thickness ranging from 0.5 m up to ten of metres. The brittle fault rocks (rich in quartz, feldspar and biotite) consist of breccia, cataclasite, foliated cataclasite and pseudotachylyte (Isık et al., 2003). Cataclasites are characterised by fractures and numerous veins rich in calcite and Fe-oxides, that destroy previous rock fabric. The percentage of clasts to matrix ratio ranges from 75 to 5%: the matrix consists of varying amounts of quartz, chlorite, Fe-oxides, sericite, epidote and carbonate (Isık et al., 2003). The top of the cataclasite consists of a discrete shear zone which includes slickensides and fibrous slickenlines of calcite or epidote (Isık et al., 2003).

2.8. The Zuccale detachment, Apennines Italy

The Zuccale fault crosscuts a lithologically heterogeneous sequence of wall rocks (Fig. 4 and Collettini and Holdsworth, 2004; Smith et al., 2007), and was active in the upper crust during intrusion of large plutonic complexes (Smith et al., 2011a). Low-angle faulting was synchronous (13–4 Ma) with the development of

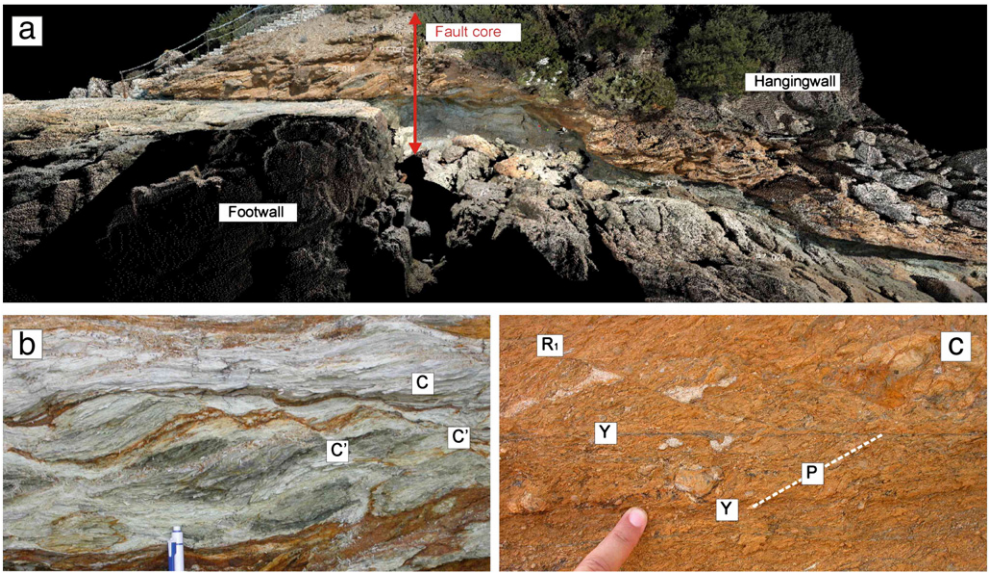

Fig. 4. a) Terrestrial laser-scanning (LIDAR) reconstruction of the ZF, Elba island, Italy (LIDAR analysis by S Smith). The fault structure is characterised by a foliated fault core separating hangingwall and footwall blocks affected by brittle faults. On this fault the red arrow is approximately 8 m long. b) Talc–smectite rich SCC' structure formed by dissolution and precipitation processes (Collettini et al., 2009a). c) YPR structure formed predominantly by cataclasis (Smith et al., 2011b).

subsidiary high-angle footwall faults and vertical veins implying slipping processes at low-dips, <20°, along the detachment in a regional stress field with vertical σ_1 (Collettini and Holdsworth, 2004; Smith et al., 2007). In the early stages of fault activity cataclasis facilitated the influx of chemically active fluids, leading to widespread syn-tectonic growth of talc, smectite and chlorite: SCC' fabric formed by dissolution precipitation processes (Fig. 4b and Collettini et al., 2009a; Smith et al., 2011b). During the later stages of fault activity, the fault rocks are represented by foliated cataclasites where deformation is accommodated by rolling and sliding of grains (quartz and dolomite) past one another along clay-lined (illite) grain boundaries (Fig. 4c and Smith et al., 2011b). The foliated cataclasites are cut by thin and striated principal slip surfaces. Veins rich in calcite and dolomite with a crack-and-seal texture formed during the fault activity suggesting local build-ups in fluid overpressure (Collettini et al., 2006).

3. Normal faults and seismicity

3.1. Dip distribution for moderate-to-large normal fault ruptures with positively discriminated slip planes

In order to investigate the dip-range of seismic ruptures in extensional environments, compilations of normal-fault dips from focal mechanisms have been published in the literature (Collettini and Sibson, 2001; Jackson and White, 1989; Thatcher and Hill, 1991). Fig. 5a is the histogram of active normal fault dips reconstructed for earthquakes with M>5.5, pure dip-slip kinematics, and positively discriminated rupture planes. To work out the ambiguity of the rupture plane in the focal mechanisms aftershock distribution and correlation with surface breaks have been used (e.g. Collettini and Sibson, 2001). Because stress perturbations induced by the main-shock may alter the regional stress field (e.g. Bohnhoff et al., 2006), in general, only main-shock ruptures have been selected in main-shock–aftershock sequences. Possible ruptures on LANF immediately following a mainshock, i.e. triggered subevents, are discussed in Axen (1999). The M>5.5 threshold means seismic ruptures larger than 5 km cutting a large part or the entire seismogenic crust. Dips are estimated principally from body-wave focal mechanisms, waveform modelling, or centroid moment tensor (CMT) analyses. Uncertainties in dip estimates range from 5° for body-wave mechanisms to 10° for techniques involving modelling of teleseismic waveforms (Molnar and Chen, 1982). The dataset presented in Fig. 5a includes data from Jackson and White (1989), Collettini and Sibson (2001) and rupture dips for East Africa (17 July, 2007, Mw = 5.9, dip = 60°, Calais et al., 2008), for the Mozambique earthquake (22 February, 2006, Mw = 7.0, dip = 70°, Yang and Chen, 2008) and for L'Aquila 2009 earthquake (6 April, 2009, Mw = 6.1, dip = 48°, Scognamiglio et al., 2010). The dip distribution for these moderate-to-large normal fault ruptures is in the range of 75–30° with no definite examples of M>5.5 normal-slip earthquakes on faults dipping less than 30°. However in the dataset (Fig. 5a), two earthquakes occurring beneath the Gulf of Corinth, Greece, nucleated on gently dipping planes (dips 30° and 33° respectively): this seismicity will be discussed in the next paragraph.

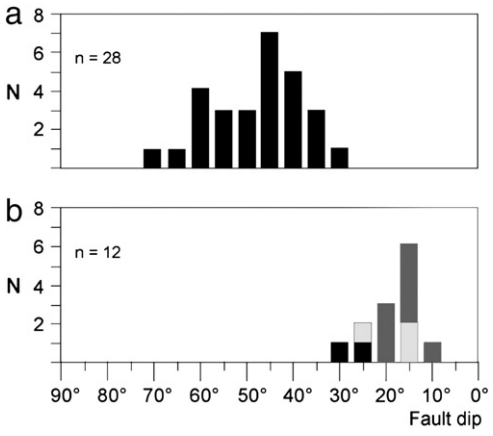

Fig. 5. a) Histogram of active normal faults dips (positively discriminated ruptures, see text for details) from compilation of Jackson and White, 1989; Collettini and Sibson, 2001 and this paper. b) Histogram of dip estimates for possible intracontinental low angle normal fault ruptures (details on Table 2). Earthquakes from Papua New Guinea, Gulf of Corinth and Northern Apennines are represented by black, heavy grey and light grey patterns respectively.

Table 2
Dip estimates for possible intracontinental low-angle normal fault ruptures.

Earthquake	Date	Magnitude	Focal depth	Dip	Reference
Woodlark	10/29/85	$M_w = 6.76$	2.7 km	24°	Abers et al., 1997.
Woodlark	1/6/1970	$M_w = 6.23$	5.3 km	32°	Abers et al., 1997.
Corinth	July–August 1991	$2.0 < M_L < 2.8$	≈9.7 km	12°	Rietbrock et al., 1996.
Corinth	July–August 1991	$2.0 < M_L < 2.8$	≈9.7 km	14°	Rietbrock et al., 1996.
Corinth	July–August 1991	$2.0 < M_L < 2.8$	≈9.7 km	14°	Rietbrock et al., 1996.
Corinth	July–August 1991	$2.0 < M_L < 2.8$	≈9.7 km	14°	Rietbrock et al., 1996.
Corinth	July–August 1991	$2.0 < M_L < 2.8$	≈9.7 km	15°	Rietbrock et al., 1996.
Corinth	July–August 1991	$2.0 < M_L < 2.8$	≈9.7 km	18°	Rietbrock et al., 1996.
Corinth	July–August 1991	$2.0 < M_L < 2.8$	≈9.7 km	20°	Rietbrock et al., 1996.
Corinth	July–August 1991	$2.0 < M_L < 2.8$	≈9.7 km	20°	Rietbrock et al., 1996.
N. Apennines	2001	$M_L \approx 1.0$ (composite)	≈5 km	15°	Chiaraluce et al., 2007
N. Apennines	2000	$M_L \approx 0.7$ (composite)	≈8 km	17°	Chiaraluce et al., 2007
N. Apennines	2000	$M_L = 1.5$	7.2 km	25°	Chiaraluce et al., 2007

3.2. Seismological data for low-angle normal faulting

Seismic activity on low-angle normal faults has been proposed in the Woodlark basin (Papua New Guinea), Gulf of Corinth (Greece) and Northern Apennines (Italy), Fig. 5b and Table 2.

In the Woodlark basin the source parameters of 16 of the largest earthquakes have been characterised using a body waveform inversion technique (Abers et al., 1997). Although in the area it is not possible to discriminate the rupture plane using the techniques mentioned above, for two of the 16 earthquakes geological data help in characterising the rupture plane (Fig. 6). In particular these two earthquakes, (events 1 and 8, with dip of 24° and 32° respectively, Fig. 6a and Table 2) show similarities for one nodal plane with the faults bounding the onshore metamorphic core complex (Abers, 1991) and with a fault imaged in a seismic reflection profile with a dip at 30° (Fig. 6b and Abers, 1991; Abers et al., 1997). An interesting aspect of the area is that the overall rate of seismic moment release is 5–20 times smaller than necessary to account for extension of the area (Abers et al., 1997), suggesting that a great amount of extension is accommodated aseismically.

In July–August 1991 a dense network of 51 seismic station operated in the western portion of the Gulf of Corinth, Greece (Fig. 7a): 774 events with $1.0 < M < 3.0$ were precisely located and 148 well-constrained focal mechanisms were obtained (Rigo et al., 1996). In cross section (Fig. 7b), at depth between 8 and 11 km, the seismicity defines a 2–5 km thick zone gently dipping northwards (Rigo et al., 1996). In this zone high-resolution cluster analysis shows earthquakes aligned along a gently north-dipping plane with shallow (12–20°) north dipping nodal planes (Fig. 7c, Table 2 and Rietbrock et al., 1996). This shallow dipping shear zone roughly corresponds to the area where the 1995 Aigion earthquake ($M_s = 6.2$, dip 33° north) nucleated (Bernard et al., 1997) and it is close to the area of the 1992 Galaxidi ($M_s = 5.9$, dip 30° north) earthquake. Rigo et al. (1996) proposed that the active fault system of the Gulf of Corinth consists of moderate to high-angle normal faults (dip 30–50°) that root into a microseismically active basal detachment. On the contrary Hatzfeld et al. (2000), on the grounds of the discrepancies between the dip-angles of the microseismicity (10–50°) and the strongest earthquakes (about 30°), proposed that the 2–5 km thick and microseismically active zone represents the seismic–aseismic transition.

In the active area of the Apennines the CROP03 deep seismic reflection profile and other commercial lines highlighted the presence of a regional low-angle normal fault, the Altotiberina fault (Barchi et al., 1998). The good correspondence between the detachment and microseismicity recorded by two high resolution seismic surveys (1987 and 2000–2001) have been documented in Boncio et al., (2000) and Chiaraluce et al. (2007). A dense network of 33 three-component seismic stations was installed for 8 months (2000–2001), in an area of ca. 70*30 km (Fig. 8 and Chiaraluce et al., 2007). The network recorded nearly 2000 earthquakes with ML<3.1. In cross sections the microseismicity defines a 0.5–1 km

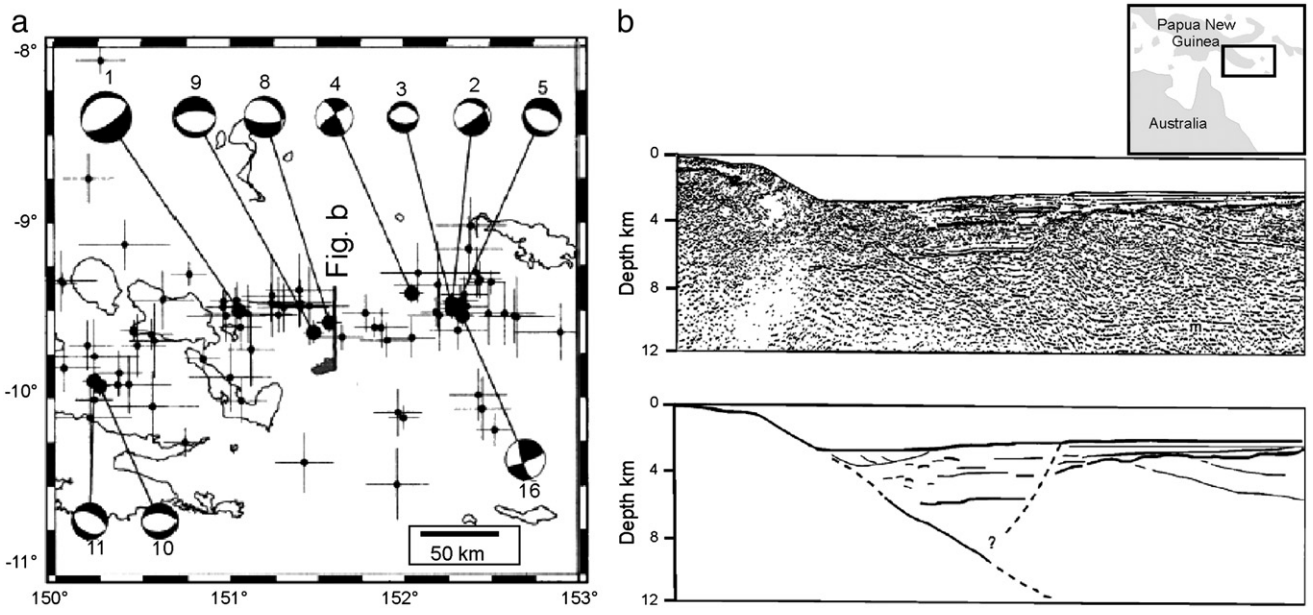

Fig. 6. a) Seismicity distribution in the Woodlark basin (Papua New Guinea) and focal mechanism (after Abers et al., 1997). b) Seismic reflection profile (see location in Fig. a) used to constrain the geometry of the faults.

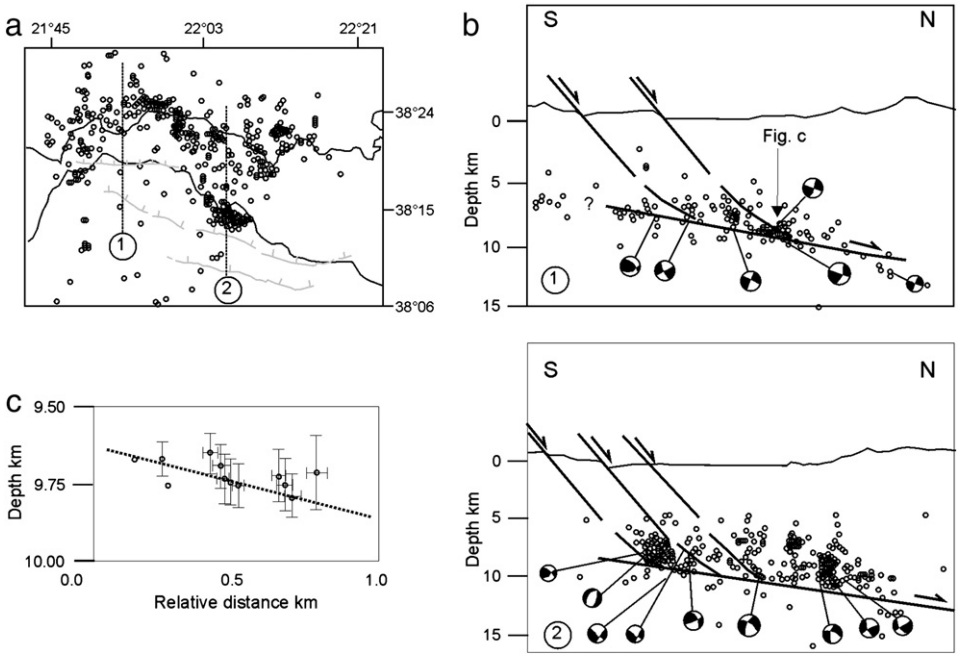

Fig. 7. a) Seismicity distribution in the Gulf of Corinth, Greece, (after Rigo et al., 1996). b) Interpretative cross sections with main faults mapped at the surface and fault plane solutions (after Rigo et al., 1996). c) Details of the microseismicity within one cluster (see location in Fig. b). The dashed line represents the inferred detachment plane obtained from a composite fault plane solution for all the events of the cluster (after Rietbrock et al., 1996).

thick fault zone, mean dip 15°, that crosscuts the upper crust from 4 km down to 16 km depth and it coincides with the low angle normal fault imaged in seismic profiles (Fig. 8). In the hanging wall block the seismicity distribution highlights minor synthetic and antithetic normal faults (4–5 km long) that sole into the detachment (Chiaraluce et al., 2007). The seismicity located along the detachment shows a constant seismicity rate, about 3 events per day $M_L \leq 2.3$, with clusters of seismicity and small earthquakes that rupture the same fault patch, i.e. repeating earthquakes. The focal mechanisms are consistent with the geometry of the fault system, and those obtained from the detachment show the same gently dipping attitude (Fig. 8, Table 2 and Chiaraluce et al., 2007).

4. Coulomb criterion and frictional reactivation for brittle faults

In an extending crust characterised by: 1) a simple extensional regime where the vertical stress is equal to the maxim principal stress, i.e. $\sigma_v = \sigma_1$ (Anderson, 1951); 2) isotropic rocks, and 3) a fluid-saturated rock mass where fluid pressure is, P_f, and effective principal stresses are $\sigma'_1 = (\sigma_1 - P_f) > \sigma'_2 = (\sigma_2 - P_f) > \sigma'_3 = (\sigma_3 - P_f)$ (Hubbert and Rubey, 1959),

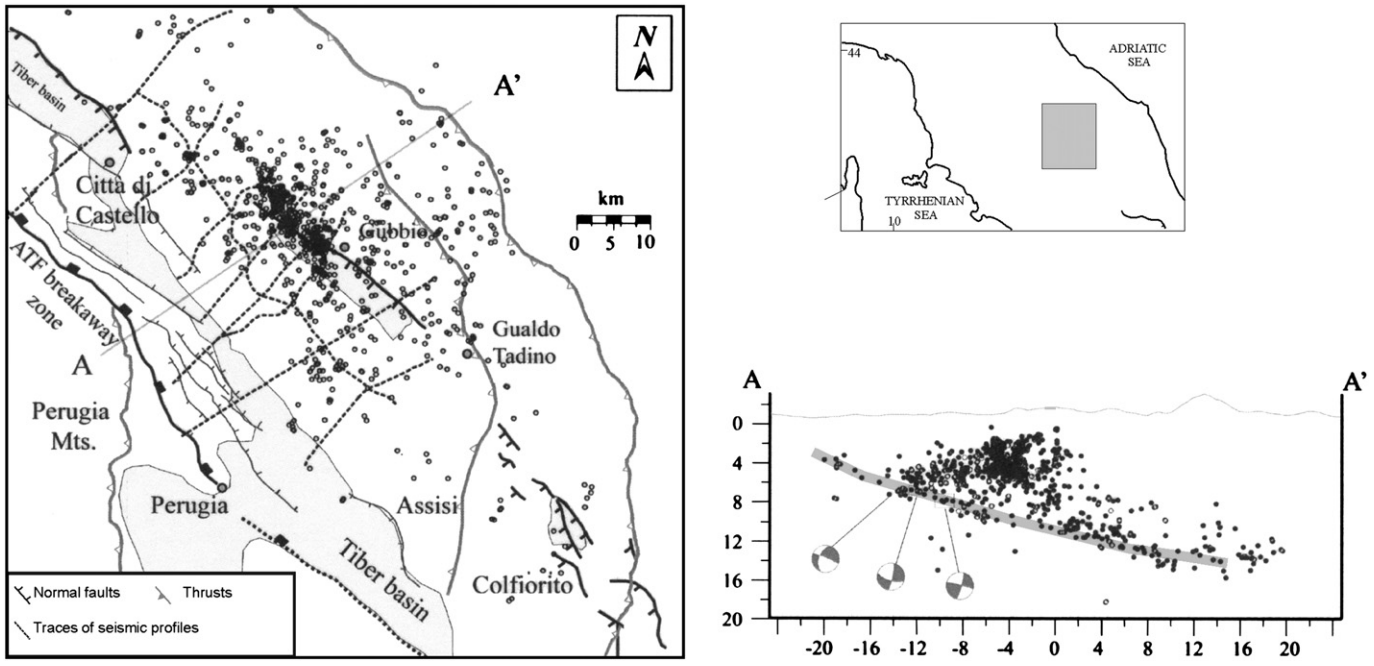

Fig. 8. Microseismicity distribution along the Altotiberina fault and in its hangingwall block (after Chiaraluce et al., 2007). Focal mechanisms of earthquakes nucleating along or near the fault show one gently dipping plane consistent with the geometry of the detachment. The grey line in the cross section represents the geometry of the low-angle normal fault as imaged by seismic reflection profiles.

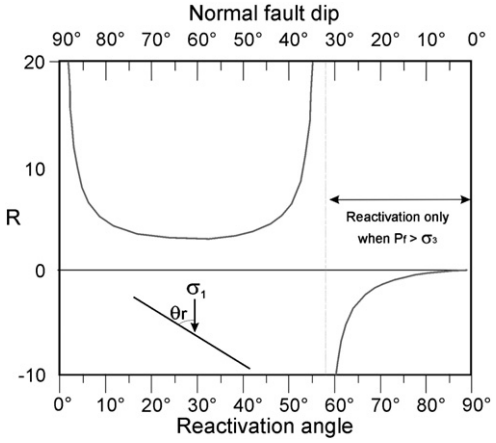

Fig. 9. Stress ratio, R, for frictional reactivation of a cohesionless fault plotted against the reactivation angle, θ_r, and normal fault dip (after Sibson, 1985).

brittle faults should form in accordance with the Coulomb criterion for shear failure (Anderson, 1951):

$$\tau = C + \mu_i(\sigma_n - P_f) \quad (1)$$

where τ and σ_n are respectively, resolved shear and normal stresses on the failure plane, C is the cohesive strength and μ_i is the coefficient of internal friction. Rock deformation experiments have shown that for a great variety of rock-types internal friction is in the range $0.5<\mu_i<1.0$ (Jaeger and Cook, 1979). Therefore brittle faults should form with angles in the range of 22–32° to σ_1 (Sibson, 1985), and in extensional environments with vertical σ_1, normal faults should initiate with dip angles in the range of 58–68° (Anderson, 1951; Sibson, 1985).

At the presence of a pre-existing discontinuity, like a mature fault, a fault formed during a previous tectonic phase or a mylonitic fabric exhumed from deeper crustal levels, re-shear of existing cohesionless faults with coefficient of sliding friction, μ, is then governed by Amontons' law:

$$\tau = \mu(\sigma_n - P_f) \quad (2)$$

Eq. (2) is critical to seismogenesis because earthquakes arise mostly from local frictional instability on existing faults (Scholz, 1998). For the two-dimensional case in which an existing fault containing the σ_2 axis lies at a reactivation angle, θ_r, to σ_1, Eq. (2) may be rewritten in terms of the effective principal stresses (Sibson, 1985) as:

$$R = (\sigma_1 - P_f)/(\sigma_3 - P_f) = (1 + \mu\cot\theta_r)/(1 - \mu\tan\theta_r) \quad (3)$$

Eq. (3) defines in 2D how easy is to reactivate a fault as a function of θ_r (Sibson, 1985): 3D frictional fault reactivation analyses are presented in (Collettini and Trippetta, 2007; Lisle and Srivastava, 2004; Morris et al., 1996). The optimal orientation for frictional reactivation, i.e. when Eq. (3) has a positive minimum (Fig. 9) is given by $\theta^*_r = 0.5\tan^{-1}(1/\mu)$. As θ_r increases or decreases away from this optimal position, the stress ratio (R) required for reactivation increases (Sibson, 2000). Frictional lock-up ($R \to \infty$) occurs when $\theta_r = 2\theta^*_r = \tan^{-1}(1/\mu)$. Beyond frictional lock-up, reshear is only possible under the tensile overpressure condition (Sibson, 2000) with $\sigma'_3 = (\sigma_3 - P_f) < 0$. The $P_f > \sigma_3$ condition is difficult to be maintained because: 1) hydrofractures form when $P_f = \sigma_3 + T$ (where T is the tensile rock strength) draining off the pressurised fluids; 2) permeability generally increases for low values of the effective stress (Patterson and Wong, 2005). It is therefore mechanically easier to form a new optimally oriented fault instead of reactivating a pre-existing one beyond the frictional lock-up (Sibson, 1985). As it is evident from Eq. (3), the frictional fault reactivation field before the frictional lockup (Fig. 9), is controlled by the frictional properties of the fault rocks. This topic will be discussed in the following discussion.

5. Discussion

5.1. Two end members fault zone structure

Field data show that most of the low-angle normal faults analysed here formed as gently dipping structures and they accommodated a significant amount of extension, also within the brittle crust, in a stress field characterised by a vertical σ_1. Fault zone structure can be represented by two end members. The first end member consists of a thick mylonitic shear zone superposed in the upper part by cataclastic processes and some localization along principal slip surfaces (e.g. Whipple, South Mountains, Tinos, Mykonos, Alaşehir). This fault zone structure represents an evolution of the shear zone from ductile to brittle during tectonic exhumation. Field data show a mylonitic footwall block with thickness ranging from 0.5 to 5 km: ductile (crystal-plasticity) deformation is generally associated to plutonic emplacement. Ductile deformation is overprinted by cataclasites, fault gouge and rare veins of pseudotachylytes, with limited lateral continuity. A planar and discrete fault surface, formed at shallow crustal levels (e.g. <3 km for the Whipple Mountains detachment), usually caps the brittle fault rocks. The second end member consists of a discrete fault core (1–20 m thick) separating hangingwall and footwall blocks affected by brittle processes (e.g. Chemehuevi-Sacramento, Zuccale, Err Nappe). The damage zone associated to these structures is characterised by fractures, small displacement faults and veins. The fault rocks within the fault core formed by diffusion mass transfer processes and/or cataclasis with grain-size reduction, rotation and translation of grains.

5.2. Detachments and fluid pressure

Structures like tensile veins or hydrofractures with crack-and-seal texture can be used to infer fluid pressure levels along exhumed faults (e.g. Secor, 1965; Sibson, 2000). Mylonites, that developed along deeper segments of detachment zones below the brittle–ductile transition, are locally accompanied by foliation parallel tensile veins that are indicative of low differential stress and high fluid pressure (Coney, 1980). In some detachments extension veins are cut by small faults that occur along the breccia zone within the detachment fault (Reynolds, 1985). These faults formed within the brittle crust in a stress field with vertical σ_1 and fracturing prevented the attainment of fluid overpressure (Axen and Selverstone, 1994; Reynolds and Lister, 1987; Townend and Zoback, 2000). Reynolds and Lister (1987) proposed two fluid-circulation systems for detachment faults: one active within the brittle crust where brittle processes prevented the attainment of fluid overpressure; another active along the deeper and ductile level of the shear zone where the sealing attitude of foliated rocks favoured the entrapment of deep-seated crustal fluids and allowed fluid overpressure. Similar conclusions have been reached for some Alpine detachments at the brittle–ductile transition (Axen et al., 2001). Although the establishment of this two fluid systems model is consistent with observations from numerous exhumed detachments, other brittle low-angle normal faults show sub-horizontal hydro-fractures in the footwall block and along the fault core. These veins testify fluid overpressures during the fault activity. These fluid overpressures are generally explained by the low permeability of the phyllosilicates documented along some detachments (Collettini et al., 2006; Manatschal, 1999; Manatschal et al., 2000). In Woodlark basin, Papua New Guinea, seismic reflection data show a detachment dipping at 25–30°. Along the detachment a 33-m-thick layer with seismic velocities of about 4.3 km s^{-1} is interpreted as serpentinite fault gouge. Along the fault gouge, isolated very low-velocity patches

Table 3
Frictional properties for different mineral phases found along exhumed low-angle normal faults. In the behaviour column, v.s. and v.w. mean velocity strengthening and weakening respectively.

Mineralogy	Friction	Mean friction	Behaviour	Lock-up	Fault dip	Reference
Granite (dry/wet)	0.5–0.8	0.65	v.s. and v.w.	57°	33°	Beeler et al., 1996; Mair and Marone, 1999; Patterson and Wong, 2005
Illite (dry)	0.42–0.68	0.55	v.s	61°	29°	Saffer and Marone, 2003; Ikari et al., 2011
Chlorite (dry)	0.7	0.7	v.s.	55°	35°	Moore and Lockner, 2004
Smectite (dry)	0.2–0.4	0.3	v.s.	73°	17°	Saffer and Marone, 2003
Talc (dry/wet)	0.23–0.05	0.11	v.s.	84°	6°	Moore and Lockner, 2008
Illite (wet)	0.25–0.4	0.33	v.s.	72°	18°	Brown et al., 2003; Ikari et al., 2009.
Chlorite (wet)	0.26–0.38	0.32	v.s.	72°	18°	Brown et al., 2003; Moore and Lockner, 2008; Ikari et al., 2009.
Smectite (wet)	<0.2	0.1	v.s.	84°	6°	Moore et al., 2010.

(V_p as low as 1.7 km s^{-1}) are interpreted as high porosities zones maintained by high fluid pressures (Floyd et al., 2001).

5.3. Fault rocks and inferred deformation mechanisms

Different fault rocks and deformation processes have been documented along detachments, depending predominantly on strain, strain-rate, confining pressure, type of fluids and protolith composition.

5.3.1. Fault gouge and foliated cataclasite with localisation

During the final stages of the fault activity, at shallow crustal levels, fault gouge or foliated cataclasites have been documented along several detachments (Chemehuevi–Sacramento, Black Mountains, Mykonos, Zuccale). The fault rocks consist of sub-rounded clasts of quartz, feldspar, carbonates within a heterogeneous fine-grained matrix. In many detachments the matrix to clast ratio increases leading to a matrix supported foliated fabric. The matrix is made of small clasts derived from the protolith (quartz, feldspar, dolomite) and new mineral phases (predominantly phyllosilicates) formed by fluid–rock interactions. Within the fault gouge and the foliated cataclasites deformation is accommodated by rolling and sliding of grains past one another favoured by the presence of a fine-grained and phyllosilicate-rich matrix (Hayman, 2006; Smith et al., 2011b). Along some detachments (Chemehuevi–Sacramento, Black Mountains, Mykonos, Zuccale) a principal slip zone with phyllosilicates (illite, smectite and kaolinite) is located at the top of the gouge.

5.3.2. Cataclasites and pseudotachylytes

In fault zones developed in quartz-feldspathic rocks, during fault exhumation, mylonites are overprinted by brittle fault rocks (e.g. Whipple, South Mountains, Mykonos, Alaşehir). The latter consist of cataclasites and ultracataclasites formed by frictional sliding and grain-size reduction. In the footwall block, fluid–rock interactions favoured the development of a chlorite-breccia. Rare veins of pseudotachylytes a few millimetres thick and up to 0.5 m long testifies slip localization and frictional melting.

5.3.3. Fluid assisted diffusion mass transfer

Whatever is the level of fluid pressure along the detachment, numerous data show that most of these structures acted as channels for crustal and deep-seated fluids. This is documented by structures in the footwall block such as: chlorite rich breccias (John and Cheadle, 2010), hydrofractures systems (Collettini et al., 2006; Manatschal, 1999; Reynolds and Lister, 1987), fluid inclusion studies of the fault zone (Famin et al., 2004). Cataclasis along the low angle normal faults increased the permeability channelling fluids into the shear zone. Fluid assisted deformation processes enhanced break-down reactions of feldspar, dolomite, serpentine, to form phyllosilicates. Increasing strain and fluid rock interaction along the detachment resulted into a switch from a clast supported fabric into a clast in matrix fabric. In clast in matrix fabric the percent of matrix is in the range of 10–70% and the main constituents of the matrix are phyllosilicates (illite, smectite, kaolinite, talc and chlorite). Phyllosilicates along some detachments form continuous networks surrounding clasts of stronger mineral phases.

5.4. Fault rocks, frictional properties and frictional fault reactivation

As discussed in paragraph 4, frictional fault reactivation is strongly controlled by fault-rock friction. Laboratory friction measurements for a wide variety of rock types have shown that with the exception of a few weak materials, fault friction, μ, is independent of rock type and lies in the range of 0.6–0.85 (Byerlee, 1978). Byerlee's friction, and in particular $\mu = 0.6$, is consistent with in situ stress measurements at crustal depths >3 km which show that faulting within the Earth's crust is controlled by optimally oriented faults possessing friction coefficients in the range $0.6 < \mu < 0.7$ with nearly hydrostatic pore pressure levels (e.g. Townend and Zoback, 2000).

In order to infer the frictional properties of the exhumed LANF presented in this review it is useful to analyse friction for the different mineralogy and rock types exposed in different outcrops (cf. paragraph 5.3). Here it will be analysed (Table 3): 1) friction at low sliding velocities, i.e. friction at quasi static condition (for dynamic weakening in friction see Di Toro et al., 2011) and 2) the velocity dependence of sliding friction, i.e. the evolution of friction following a velocity step (e.g. Dieterich and Kilgore, 1994; Marone, 1998; Scholz, 1998). The velocity dependence of friction is relevant to infer the seismic behaviour of brittle faults. For a step change in sliding velocity from V_0 to V (Fig. 10), if friction increases with increasing sliding velocity, this indicates a velocity strengthening behaviour that results in stable fault sliding and is associated with aseismic fault creep; if

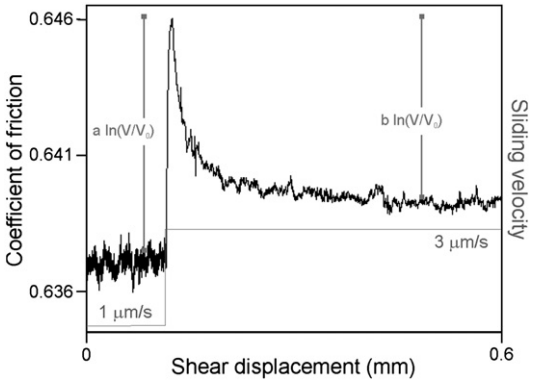

Fig. 10. Evolution in friction for a velocity step from 1 (V_0) to 3 (V) μm/s. The instantaneous change in friction coefficient scales as the friction parameter $a \ln(V/V_0)$. The decay to a new steady state scales as the friction parameter $b \ln(V/V_0)$. Frictional velocity dependence is defined as: $(a-b) = [\Delta\mu_{ss}/\ln(V/V_0).]$, where $\Delta\mu_{ss}$ is the change in the steady state coefficient of friction upon an instantaneous change in sliding velocity from V_0 to V. Positive values of (a–b) indicate velocity strengthening frictional behaviour, negative values of (a–b) indicate velocity-weakening frictional behaviour (details in Dieterich and Kilgore, 1994; Marone, 1998; Scholz, 1998).

friction decreases this indicates a velocity-weakening behaviour that is a prerequisite for unstable, stick–slip behaviour associated with earthquake nucleation (Dieterich and Kilgore, 1994; Marone, 1998; Scholz, 1998).

For cataclasites and ultracataclasites composed of quartz and feldspar (e.g. Whipple, South Mountains, Chemehuevi–Sacramento, Mykonos, Alaşehir), laboratory experiments constrain friction in the range of 0.5–0.8 (Beeler et al., 1996; Mair and Marone, 1999; Patterson and Wong, 2005). The velocity dependence of friction evolves from velocity strengthening to weakening with increasing displacement and localization (Beeler et al., 1996; Mair and Marone, 1999).

For gouge, foliated gouge and cataclasites (e.g. Chemehuevi-Sacramento, Black Mountains, Mykonos, Zuccale) the frictional properties of the fault rocks are controlled by the percent of weak mineral phases, and more than 50% of the weak mineral phase is required for fault weakness (Numelin et al., 2007; Saffer and Marone, 2003). For 50% smectite–quartz mixture, at normal stress >20 MPa and in dry experiments, friction is in the range of 0.2–0.4 and the behaviour is predominantly velocity strengthening (Saffer and Marone, 2003). Smectite wet is significantly weaker $\mu<0.2$ (Moore et al., 2010). Dry illite shows a friction of 0.42–0.68 and a velocity strengthening behaviour (Ikari et al., 2011; Saffer and Marone, 2003) and wet illite is significantly weaker, $\mu=0.27$–0.32 (Brown et al., 2003; Ikari et al., 2009) and velocity strengthening (Ikari et al., 2009). Dry chlorite is strong with $\mu\approx0.7$, whereas wet chlorite has a friction in the range of 0.26–38 (Brown et al., 2003; Ikari et al., 2009; Moore and Lockner, 2008) and is velocity strengthening (Ikari et al., 2009).

The frictional properties of two LANF have been recently tested. Most of the samples (granular material) collected from a LANF in Panamint Valley, California, show friction in the range of 0.6–0.7 (Numelin et al., 2007), and only a few samples with greater than 50% total clay content are weaker ($\mu=0.2$–0.4). The fault gouge and the cataclasites of the upper portion of the Zuccale fault are characterised by $\mu>0.6$ and only fault zone portions rich in chlorite and kaolinite show friction in the range of 0.4–0.5 (Smith and Faulkner, 2010). Fault rocks from both detachments are characterised by a velocity strengthening behaviour (Numelin et al., 2007; Smith and Faulkner, 2010). Along some detachments (e.g. Err Nappe, the basal horizon of the Zuccale fault) fluid assisted diffusion mass transfer generate fault rocks consisting of continuous networks rich in phyllosilicates (talc, chlorite, smectite). Friction experiments conducted on fault rocks sheared under their in situ geometry show that fault weakness can occur in cases where weak mineral phases constitute only a small percent of the total fault rock (Collettini et al., 2009b). For the foliated basal horizon of the Zuccale fault, friction is in the range of 0.2–0.3 and the behaviour is velocity strengthening (Collettini et al., 2009b).

Now I will integrate fault rocks and associated/inferred frictional properties with frictional fault reactivation theory in order to investigate the reactivation field of normal faults (Fig. 11). The analysis is based on the assumption that the regional maximum compressive stress, σ_1, is vertical. In the mechanical analysis it is important to highlight that in order to apply the friction coefficients of the mineral phases reported in Table 3, the specific mineral phase has to be greater than 50 wt.% for granular fault rocks and 20–30 wt.% for continuous networks of weak minerals.

In dry conditions frictional reactivation theory cannot explain movements on detachments made of quartz-feldspar, chlorite and illite. Only fault zone rich in smectite and talc can be reactivated with dip <20° (Fig. 11 and Table 3). However low-angle normal faults

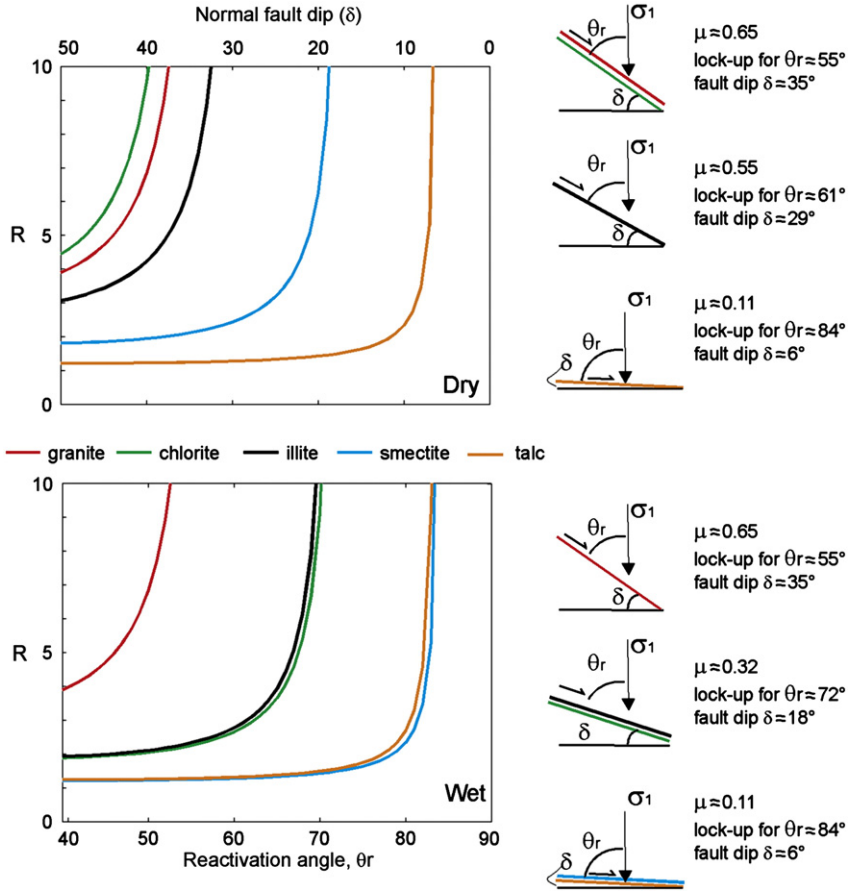

Fig. 11. Stress ratio, R, for frictional reactivation of a cohesionless fault plotted against the reactivation angle, θ_r and normal fault dip (after Sibson, 1985). Frictional lock-up ($R\rightarrow\infty$) and corresponding normal fault dip for fault zone characterised by different mineralogy, under dry/wet conditions cf. also Table 3.

represent channels for crustal fluids and therefore frictional properties at wet conditions are more appropriate. Quartz-feldspathic, wet cataclasites do not allow movements on normal faults dipping less than 27–39°. In wet conditions the frictional lock-up angle for normal faults rich in chlorite and illite is at ≈72°, implying that detachments can be reactivated with dip-angles up to 18° at the presence of a great amount of chlorite and illite. In addition, some fluid overpressure is required in order to reactivate faults close to the frictional lock-up angle: the reactivation parameter, R, goes to infinity in Eq. 3, only if P_f is close to σ_3 (Sibson, 1985). Faults rich in smectite and talc are very weak and frictional reactivation can occur along faults dipping even close to 0° (Fig. 11 and Table 3).

With the exception of the granite cataclasite affected by slip localization, all the phyllosilicate-rich fault rocks are characterised by a velocity strengthening behaviour, resulting in stable sliding and fault creep. However a seismic rupture nucleated on a neighbouring fault may propagate at high sliding velocity along the phyllosilicate-rich horizons (e.g. Boutareaud et al., 2008; Niemeijer and Spiers, 2006).

5.5. Frictional fault reactivation and seismicity

The dip distribution for positively discriminated normal-slip ruptures extends over the range 75°>δ>30°, with a peak at 45° (Fig. 5a). This peak can reflect the orientation of deeper and ductile shear zones following planes of maximum shear stress, i.e. formed at 45° to the σ_1 in the ductile crust (e.g. De Paola et al., 2008; Thatcher and Hill, 1991) and then reactivated within the brittle crust during exhumation. No positively discriminated (cf. paragraph 3.1) normal-slip earthquakes on faults dipping less than 30° are confirmed. Interpretation of these dip distributions depends critically on whether σ_1 is indeed vertical in an extending crust. If such is the case, the apparent cutoff of the seismicity at $\theta_r \approx 60°$ is consistent with frictional lock-up for $\mu_s = 0.6$, at the bottom of Byerlee (1978) friction range (e.g. Collettini and Sibson, 2001), if σ_1 is not vertical the apparent frictional lockup at $\theta_r \approx 60°$ would then be fortuitous.

For the two major earthquakes, with geological constraints, recorded in Papua New Guinea (cf. paragraph 3) the fault dip is 32° and 24° respectively (Fig. 6 and Table 2). These earthquakes can be explained as ruptures close to the frictional lock-up for friction close to 0.5–0.6 and favoured by the fluid overpressure documented along the detachment (Floyd et al., 2001). In addition, talc-rich serpentinites have been drilled along some exposed fault zones of the area with a low friction of 0.21–0.3 (Kopf and Brown, 2003). The presence of talc and serpentinites can reduce the average frictional strength of the detachment and their velocity strengthening behaviour can explain the great amount of extension that in the area is accommodated aseismically (Abers et al., 1997). In this interpretation the larger earthquakes of the area would represent ruptures close to frictional lock-up (favoured by fluid overpressure) nucleating along wide locked patches that are interdispersed within a creeping fault zone.

In the Gulf of Corinth, most of the microseismicity is located at 8–11 km depth along a gently dipping (12–20°) deformation zone (Rietbrock et al., 1996; Rigo et al., 1996). Major earthquakes nucleate from this zone with dip of 33°, the 1995 Aigion earthquake (Ms = 6.2), and 30°, the 1992 Galaxidi (Ms = 5.9) earthquake. The LANF documented in the Cyclades, e.g. Tinos and Mykonos detachments, may represent ancient and exhumed analogues of the currently active faults beneath the Gulf of Corinth (e.g. Jolivet, 2010; Lecomte, 2010). Outcrop exposures in the Cyclades document a thick (several km), gently dipping and ductile shear zone with some localization in the upper part: higher angle normal faults sole into the detachment (cf. paragraph 2). Enbrittlement, induced by fluid overpressure and/or increase in strain-rate (e.g. Goodwin, 1999) or asperities along the ductile shear zone (e.g. Fagereng and Sibson, 2010; Faulkner et al., 2003) can be responsible for the microseismicity. Major earthquakes would be associated to the moderate-to-high angle faults that sole into the detachment.

In the Apennines the Altotiberina low-angle normal fault (mean dip 15°) is characterised by aseismic creep and microseismicity (Chiaraluce et al., 2007; Hreinsdottir and Bennett, 2009). The Zuccale low-angle normal fault, belonging to the same fault system, represents an exhumed analogue. Frictional properties of the fault rocks suggest stable slips on a weak (μ<0.3) detachment induced by the development of phyllosilicates coupled with fluid overpressure (Collettini et al., 2009a; Smith and Faulkner, 2010). Stable slip promoted by velocity strengthening materials can be a possible explanation for the great amount of slip accommodated aseismically along the Altotiberina fault (e.g. Chiaraluce et al., 2007; Collettini and Holdsworth, 2004; Hreinsdottir and Bennett, 2009). Fluid overpressures associated to brittle faulting can be a possible explanation for microseismicity (Collettini and Barchi, 2002).

6. Open questions

Geological data collected for detachments developed in different extensional provinces worldwide imply that low-angle normal faults are common structures and they are important for accommodating crustal extension in a stress field with a vertical σ_1, also within the brittle crust. If we trust these geological data two mechanical problems have not been solved yet.

The first one regards the possibility that moderate-to-large earthquakes may nucleate on low-angle normal faults. In order to explain movements on LANF we can invoke specialised conditions like the massive presence of phyllosilicates along detachments coupled with some fluid overpressure: the low friction coefficient of the phyllosilicates can explain movements on faults at high angle to σ_1 and the velocity strengthening behaviour of the phyllosilicates implies fault creep and therefore can be used to explain the absence of moderate-to-large earthquakes on gently dipping planes in seismological records. However a widespread development of phyllosilicates does not seem to be a common feature for most of the exhumed detachments (paragraph 2 and Table 1). At the same time some LANF are characterised by principal slip planes where slip is localised along thin layers of cataclasites, other detachments show granitic cataclasites and ultracataclasites with shear localization associated with, although rare, pseudotachylyte production. These fault rocks are the typical structures of the brittle crust where a great amount of deformation is accommodated seismically (Scholz, 1998). These data suggest that slip on low-angle normal faults can be seismic and a possible explanation for the absence of large ruptures on LANF in the contemporary seismic records can be attributable to their having unusually long recurrence intervals (Wernicke, 1995). I think that the integration of field, seismological and mechanical data does not highlight a simple mechanical explanation that can answer the question as to whether normal faults may generate moderate to large earthquakes at very low dips in the upper continental crust. This open question shares many similarities with the mechanical paradox of the San Andreas fault in California. The San Andreas, like low-angle normal faults, moves although oriented at high angle to the regional σ_1 (Zoback et al., 1987). The fault is characterised by locked portions hosting the strongest earthquakes and a creeping section (e.g. Moore and Rymer, 2007). Along the creeping section a scientific borehole penetrated the active portion of the fault zone at about 3 km depth (Zoback et al., 2010). The active fault portion is rich in phyllosilicates (talc and smectite) with friction <0.2 and a velocity strengthening behaviour (Carpenter et al., 2011; Moore et al., 2010; Moore and Rymer, 2007): these data well explain the weakness of the fault and its creeping behaviour, however they cannot explain the moderate to large earthquakes occurring along the locked portions of the San Andreas fault oriented at high angles to the regional σ_1.

The second open question regards how normal faults initiate with low dips within the brittle continental crust. Although some brittle detachments are made of cataclasites that reworked and reactivated pre-existing ductile (crystal plasticity) shear zones, other LANF (e.g. Chemehuevi-Sacramento, Zuccale, Err Nappe) formed as gently dipping structures within a brittle crust characterised by a vertical σ_1. To explain the initiation of these structures it is not possible to invoke stress rotation near the brittle ductile transition (e.g. Melosh, 1990; Westaway, 1999; Yin, 1989) since these structures are within the brittle crust. At the same time stress rotation induced by: a) a weak fault core sandwiched in a strong crust (e.g. Axen, 1992) or b) a fractured damage zone affected by changes in elastic properties (Faulkner et al., 2006), are unlikely since at fault initiation no fault core nor damage zone are present. The influence of rock anisotropy in the mechanics of faulting (e.g. Healy, 2009) and in fault initiation may represent a promising road for solving this mechanical problem.

In conclusion, the specialised conditions that we have to invoke to explain movements on low-angle normal faults together with the difficulty to explain the initiation of some of these structures conflict with the geological observation that low-angle normal faults are common structures in extensional environments. In my view more field data, aimed to characterise mineralogical and textural evolution of fault zones, innovative laboratory experiments coupled with high resolution seismological data and mechanical models are needed to solve this long lasting issue in geology and geophysics.

Acknowledgments

This research was supported by the ERC St.G. Nr. 259256 GLASS project. I thank M. Barchi, F. Mirabella, F. Trippetta and S. Smith for comments on an early version of the manuscript. L. Chiaraluce, D. Cowan, L. Goodwin, L. Jolivet, E. Lecomte and A. Rietbrock provided some details on published data and material presented in this review. B. John and an anonymous reviewer provided critical reviews, which significantly improved the paper.

References

Abers, G.A., 1991. Possibles eismogenics hallow-dipping normal faults in the Woodlark-D'Entrecasteaux extensional province, Papua New Guinea. Geology 19, 1205–1208.
Abers, G.A., 2009. Slip on shallow-dipping normal faults. Geology 37, 767–768.
Abers, G.A., Mutter, C.Z., Fang, J., 1997. Shallow dips of normal faults during rapid extension: earthquakes in the Woodlark-D'Entrecasteaux rift system, Papua New Guinea. Journal of Geophysical Research 102, 15301–15317.
Anderson, E.M., 1951. The Dynamics of Faulting, 2nd edition. Oliver and Boyd, Edinburgh, p. 206.
Anderson, R.E., 1971. Thin-skin distention in the Tertiary rock of southwestern Nevada. Geological Society of America Bulletin 105, 1019–1052.
Axen, G.J., 1992. Pore pressure, stress increase, and fault weakening in low-angle normal faulting. Journal of Geophysical Research 97, 8979–8991.
Axen, G.J., 1999. Low-angle normal fault earthquakes and triggering. Geophysical Research Letters 26 (24), 3693–3696. doi:10.1029/1999GL005405.
Axen, G.J., 2004. Mechanics of low-angle normal faults. In: Karner, G.D., Morris, J.D., Driscoll, N.W., Silver, E.A. (Eds.), Rheology and Deformation of the Lithosphere at Continental Margins: MARGINS Theoretical and Experimental Earth Science Series, pp. 46–91.
Axen, G., Selverstone, J., 1994. Stress state and fluid pressure levels on the Whipple detachment fault, California. Geology 22 838-838.
Axen, G.J., Selverstone, J., Wawrzyniec, T., 2001. High-temperature embrittlement of extensional Alpine mylonite zones in the midcrustal ductile–brittle transition. Journal of Geophysical Research 106, 4337–4348.
Barchi, M.R., Minelli, G., Pialli, G., 1998. The CROP 03 profile: a synthesis of results on deep structures of the Northern Apennines. Memorie della Società Geologica Italiana 52, 383–400.
Beeler, N.M., Tullis, T.E., Blanpied, M.L., Weeks, J.D., 1996. Frictional behaviour of large displacement experimental faults. Journal of Geophysical Research 101, 8697–8715.
Bernard, P., 27 others, 1997. The Ms = 6.2, June 15, 1995 Aigion earthquake (Greece): evidence for low angle normal faulting in Corinth rift. Journal of Seismology 1, 131–150.
Bohnhoff, M., Grosser, H., Dresen, G., 2006. Strain partitioning and stress rotation at the North Anatolian fault zone from aftershock focal mechanisms of the 1999 Izmit Mw = 7.4 earthquake. Geophysical Journal International 166, 372–385.
Boncio, P., Brozetti, F., Lavecchia, G., 2000. Architecture and seismotectonics of a regional low-angle normal fault zone in central Italy. Tectonics 19, 1038–1055.
Bos, B., Spiers, C.J., 2001. Experimental investigation into the microstructural and mechanical evolution of phyllosilicate-bearing fault rock under conditions favouring pressure solution. Journal of Structural Geology 23, 1187–1202.
Boutareaud, S., et al., 2008. Clay-clast aggregates: a new textural evidence for seismic fault sliding? Geophysical Research Letters 35, L05302. doi:10.1029/2007GL032554.
Brown, K.M., Kopf, A., Underwood, M.B., Weinberger, J.L., 2003. Compositional and fluid pressure controls on the state of stress on the Nankai subduction thrust: a weak plate boundary. Earth and Planetary Science Letters 214, 589–603.
Byerlee, J.D., 1978. Friction of rocks. Pure and Applied Geophysics 116, 615–626.
Calais, E., 15 others, 2008. Strain accommodation by slow slip and dyking in a youthful continental rift, East Africa. Nature 456, 783–787.
Carpenter, B.M., Marone, C., Saffer, D.M., 2011. Weakness of the San Andreas Fault revealed by samples from the active fault zone. Nature Geoscience 4, 251–254. doi:10.1038/ngeo1089.
Chester, F.M., Friedman, M., Logan, J.M., 1985. Foliated cataclasites. Tectonophysics 111, 139–146.
Chiaraluce, L., Chiarabba, C., Collettini, C., Piccinini, D., Cocco, M., 2007. Architecture and mechanics of an active low-angle normal fault: Alto Tiberina Fault, northern Apennines, Italy. Journal of Geophysical Research 112, B10310. doi:10.1029/2007JB005015.
Collettini, C., Barchi, M.R., 2002. A low angle normal fault in the Umbria region (Central Italy): a mechanical model for the related microseismicity. Tectonophysics 359, 97–115.
Collettini, C., Holdsworth, R.E., 2004. Fault zone weakening processes along low-angle normal faults: insights from the Zuccale Fault, Isle of Elba, Italy. Journal of the Geological Society 161, 1039–1051.
Collettini, C., Sibson, R.H., 2001. Normal faults normal friction? Geology 29, 927–930.
Collettini, C., Trippetta, F., 2007. A slip tendency analysis to test mechanical and structural control on aftershock rupture planes. Earth and Planetary Science Letters 255, 402–413.
Collettini, C., De Paola, N., Goulty, N.R., 2006. Switches in the minimum compressive stress direction induced by overpressure beneath a low-permeability fault zone. Terra Nova 18, 224–231.
Collettini, C., Viti, C., Smith, S.F.A., Holdsworth, R.E., 2009a. The development of interconnected talc networks and weakening of continental low-angle normal faults. Geology 37, 567–570.
Collettini, C., Niemeijer, A., Viti, C., Marone, C.J., 2009b. Fault zone fabric and fault weakness. Nature 462, 907–910.
Coney, P.G., 1980. Cordilleran metamorphic core complexes — an overview. In: Crittenden Jr., M.D., et al. (Ed.), Cordilleran Metamorphic Core Complexes: Geological Society of America Memoir, 153, pp. 7–31.
Cowan, D.S., Cladouhos, T.T., Morgan, J., 2003. Structural geology and kinematic history of rocks formed along low-angle normal faults, Death Valley, California. Geological Society of America Bulletin 115, 1230–1248.
Davis, G.A., 1986a. Upward transport of mid-crustal mylonitic gneisses in the footwall of a Miocene detachment fault, Whipple Mountains, southeastern California. Geological Society of America Abstract 18, 98.
Davis, G.H., 1986b. Shear-zone model for the origin of metamorphic core complexes. Geology 11, 342–347. doi:10.1130/0091-7613(1983.
Davis, G.A., 1988. Rapid upward transfer of mid-crustal mylonitic gneisses in the footwall of a Miocene detachment fault, Whipple Mountains, southern California. Geologische Rundschau 77, 191–209.
Davis, G.A., Lister, G.S., Reynolds, S.J., 1986. Structural evolution of the Whipple and South Mountains shear zones, southwestern United States. Geology 14, 7–10.
De Paola, N., Collettini, C., Faulkner, D.R., Trippetta, F., 2008. Fault zone architecture and deformation processes within evaporitic rocks in the upper crust. Tectonics vol. 27. doi:10.1029/2007TC002230 (ISSN: 0278–7407).
Di Toro, G., Han, R., Hirose, T., De Paola, N., Nielsen, S., Mizoguchi, K., Cocco, M., Shimamoto, T., 2011. Fault lubrication during earthquakes. Nature 471, 494–497.
Dieterich, J.H., Kilgore, B., 1994. Direct observation of frictional contacts: new insights for state dependent properties. Pure and Applied Geophysics 143, 283–302.
Drewes, H., 1963. Geology of the Funeral Peak Quadrangle, California, on the eastern flank of Death Valley. U. S. Geological Survey Professional Paper 413, 78.
Drury, M.R., Urai, L.J., 1990. Deformation related recrystallisation processes. Tectonophysics 172, 235–253.
Fagereng, A., Sibson, R.H., 2010. Melange rheology and seismic style. Geology 38, 751–754.
Famin, V., Philippot, P., Jolivet, L., Agard, P., 2004. Evolution of hydrothermal regime along a crustal shear zone, Tinos Island, Greece. Tectonics 23, TC5004. doi:10.1029/2003TC001509.
Faulkner, D.R., Lewis, A.C., Rutter, E.H., 2003. On the internal structure and mechanics of large strike-slip faults: field observations from the Carboneras fault, southeastern Spain. Tectonophysics 367, 235–251.
Faulkner, D.R., Mitchell, T.M., Healy, D., Heap, M.J., 2006. Slip on 'weak' faults by the rotation of regional stress in the fracture damage zone. Nature 444, 922–925.
Floyd, J., Mutter, J., Goodliffe, A.M., Taylor, B., 2001. Evidence for fault weakness and fluid flow within an active low-angle normal fault. Nature 411, 779–783.
Gessner, K., Ring, U., Johnson, C., Hetzel, R., Passchier, C.W., Gungor, T., 2001. An active bivergent rolling-hinge detachment system: central Menderes metamorphic core complex in western Turkey. Geology 29, 611–614.
Goodwin, L.B., 1999. Controls on pseudotachylytes formation during tectonic exhumation in the South Mountains metamorphic core complex, Arizona. In: Ring, U., Brandon, M.T., Lister, G.S., Willet, S.D. (Eds.), Exhumation processes: normal faulting, ductile flow and erosion: Geological Society, London, Special Publications, 154, pp. 325–342.

Hatzfeld, D., Karakostas, V., Ziazia, M., Kassaras, I., Papadimitriou, E., Makropoulos, K., Voulgaris, N., Papaioannou, C., 2000. Microseismicity and faulting geometry in the Gulf of Corinth (Greece). Geophysical Journal International 141, 438–456.
Hayman, N.W., 2006. Shallow crustal rocks from the Black Mountains detachments, Death Valley, CA. Journal of Structural Geology 28, 1767–1784.
Hayman, N.W., Knott, J.R., Cowan, D.S., Nemser, E., Sarna-Wojcicki, A., 2003. Quaternary low-angle slip on detachment faults in Death Valley, California. Geology 31, 343–346.
Healy, D., 2009. Anisotropy, pore fluid pressure and low angle normal faults. Journal of Structural Geology 31, 561–574. doi:10.1016/j.jsg.2009.03.001.
Hirth, G., Tullis, J., 1992. Dislocation creep regimes in quartz aggregates. Journal of Structural Geology 14, 145–159.
Howard, K.A., John, B.E., 1987. Crustal extension along a rooted system of imbricate low-angle faults: Colorado River extensional corridor, California and Arizona. In: Coward, M.P., Dewey, J.F., Hancock, P.L. (Eds.), Continental extensional tectonics: Geological Society of London Special Publication, 28, pp. 299–311.
Hreinsdottir, S., Bennett, R.A., 2009. Active aseismic creep on the Alto Tiberina low-angle normal fault, Italy. Geology 37, 683–686.
Hubbert, M.K., Rubey, W.W., 1959. Role of fluid overpressure in mechanics of overthrust faulting. Geological Society of America Bulletin 70, 583–586.
Ikari, M.J., Saffer, D.M., Marone, C., 2009. Frictional and hydrologic properties of clay-rich fault gouge. Journal of Geophysical Research 114, B05409. doi:10.1029/2008JB006089.
Ikari, M.J., Saffer, D.M., Marone, C., 2011. On the relation between fault strength and frictional stability. Geology 39, 83–86.
Imber, J., Holdsworth, R.E., Butler, C.A., 2001. A reappraisal of the Sibson-Scholz fault zone model: the nature of the frictional to viscous ("brittle–ductile") transition along a long-lived, crustal scale fault, Outer Hebrides, Scotland. Tectonics 20, 601–624.
Isık, V., Seyitoglu, G., Cemen, I., 2003. Ductile–brittle transition along the Alasehir detachment fault and its structural relationship with the Simav detachment fault, Menderes massif, western Turkey. Tectonophysics 374, 1–18.
Jackson, J.A., White, N.J., 1989. Normal faulting in the upper continental crust: observations from regions of active extension. Journal of Structural Geology 11, 15–36.
Jaeger, J.G., Cook, N.G.W., 1979. Fundamentals of Rock Mechanics, 3rd edition. Chapman and Hall, London, p. 585.
John, B.E., 1987. Geometry and evolution of a mid-crustal extensional fault system: Chemehuevi Mountains, southeastern California. Geological Society of London Special Publication 28, 313–335.
John, B.E., Cheadle, M.J., 2010. Deformation and alteration associated with oceanic and continental detachment fault systems: are they similar? In: Rona, Devey, Dyment, Murton (Eds.), Diversity of Hydrothermal Systems on Slow-spreading Ocean Ridges, AGU Monograph, pp. 175–205.
John, B.E., Foster, D.A., 1993. Structural and thermal constraints on the initiation angle of detachment faulting in the southern Basin and Range: the Chemehuevi Mountains case study. Geological Society of America Bulletin 105, 1091–1108. doi:10.1130/0016-7606(1993) 105.
Jolivet, L., 2010. A comparison of strain pattern in the Aegean, geodynamic implications. Earth and Planetary Science Letters 187, 95–104.
Jolivet, L., Lecomte, E., Huet, B., Denèle, Y., Lacombe, O., Labrousse, L., Le Pourhiet, L., Mehl, C., 2010. The North Cycladic detachment system. Earth and Planetary Science Letters 289, 87–104. doi:10.1016/j.epsl.2009.10.032.
Katzir, Y., Matthews, A., Garfunkel, Z., Schliestedt, M., Avigad, D., 1996. The tectonometamorphic evolution of a dismembered ophiolite (Tinos, Cyclades, Greece). Geological Magazine 133, 237–254.
Kopf, A., Brown, K.M., 2003. Friction experiments on saturated sediments and their implications for the stress state of the Nankai and Barbados subduction thrusts. Marine Geology 202, 193–210.
Lecomte, E., 2010. Détachements et failles à faible pendage : Cinématique et localisation de la déformation,approche de terrain et modélisation numérique. Exemples des Cyclades. Docteur de l'Université Pierre et Marie Curie - Paris VI, p. 301.
Lecomte, E., Jolivet, L., Lacombe, O., Denèle, Y., Labrousse, L., Le Pourhiet, L., 2010. Geometry and kinematics of Mykonos detachment, Cyclades, Greece: evidence for slip at shallow dip. Tectonics 29, TC5012. doi:10.1029/2009TC002564.
Lisle, R.J., Srivastava, D.C., 2004. Test of the frictional reactivation theory for faults and validity of fault-slip analysis. Geology 32, 569–572.
Lister, G.S., Davis, G.A., 1989. The origin of metamorphic core complexes and detachment faults formed during Tertiary continental extension in the northern Colorado River region, U.S.A. Journal of Structural Geology 11, 65–94.
Livaccari, L.F., Geissman, J.W., Reynolds, S.-J.-., 1993. Palaeomagnetic evidence for large-magnitude, low-angle normal faulting in a metamorphic core complex. Nature 361, 56–59.
Longwell, C.R., 1945. Low-angle normal faults in the Basin and Range province. Transactions of the American Geophysical Union 26, 107–118.
Mair, K., Marone, C., 1999. Friction of simulated fault gouge for a wide range of velocities and normal stresses. Journal of Geophysical Research 104, 28,899–28,914.
Manatschal, G., 1999. Fluid-and reaction-assisted low-angle normal faulting: evidence from rift-related brittle fault rocks in the Alps (Err nappe, eastern Switzerland). Journal of Structural Geology 21, 777–793.
Manatschal, G., Nievergelt, P., 1997. A continent-ocean transition recorded in the Err and Platta nappes (Eastern Switzerland). Eclogae Geologicae Helvetiae 90, 3–27.
Manatschal, G., Marquer, D., Früh-Green, G.L., 2000. Channelized fluid flow and mass transfer along a rift-related detachment fault (Eastern Alps, southeastern Switzerland). Geological Society of America Bulletin 112 (1), 21–33.
Marone, C., 1998. Laboratory-derived friction laws and their application to seismic faulting. Annual Review of Earth and Planetary Sciences 26, 643–696.
Melosh, H.J., 1990. Mechanical basis for low-angle normal faulting in the Basin and Range province. Nature 343, 331–335.
Molnar, P., Chen, W.-P., 1982. Seismicity and mountain building. In: Hsu, K.J. (Ed.), Mountain building processes. Academic Press, London, pp. 41–57.
Moore, D.E., Lockner, D.A., 2008. Talc friction in the temperature range 25°-400° C: Relevance for fault-zone weakening. Tectonophysics 449, 120–132. doi:10.1016/j.tecto.2007.11.039.
Moore, D.E., Rymer, M., 2007. Talc-bearing serpentinites and the creeping section of the San Andreas fault. Nature 448, 795–797. doi:10.1038/nature06064.
Moore, D.E., Lockner, D.A., Hickman, S., Rymer, M.J., 2010. Very low strength fault gouge of metasomatic origin in the two actively creeping strands at SAFOD, Parkfield, California, USA. In: Di Toro, et al. (Ed.), Physico-chemical processes in seismic faults: Padova, pp. 50–51.
Morris, A., Ferrill, D.A., Henderson, D.B., 1996. Slip-tendency analysis and fault reactivation. Geology 24, 275–278.
Niemeijer, A.R., Spiers, C.J., 2006. Velocity dependence of strength and healing behaviour in simulated phyllosilicate-bearing fault gouge. Tectonophysics 427, 231–253.
Numelin, T., Marone, C., Kirby, E., 2007. Frictional properties of natural fault gouge from a low-angle normal fault, Panamint Valley, CA. Tectonics TC2004. doi:10.1029/2005TC001916.
Patterson, M.S., Wong, T.F., 2005. Experimental Rock Deformation — The Brittle Field, 2nd ed. Springer-Verlag, Berlin, Heidelberg, New York, p. 348.
Proffett, J.M., 1977. Cenozoic geology of the Yerington district, Nevada, and implications for the nature of Basin and Range faulting. Geological Society of America Bulletin 88, 247–266.
Reynolds, S.J., 1985. Geology of the South Mountains, Central Arizona. Arizona Bureau of Geology and Mineral technology. Geological Survey Bulletin 195.95.
Reynolds, S.J., Lister, G.S., 1987. Structural aspects of fluid–rock interactions in detachment zones. Geology 15, 362–366.
Reynolds, S.J., Shafiqullah, M., Damon, P.E., De Witt, E., 1986. Early Miocene mylonitization and detachment faulting, South Mountains, central Arizona. Geology 14, 283–286.
Rietbrock, A., Tiberi, C., Scherbaum, F., Lyon-Caen, H., 1996. Seismic slip on a low-angle normal fault in the Gulf of Corinth: evidence from high-resolution cluster analysis of microearthquakes. Geophysical Research Letters 23, 1817–1820.
Rigo, A., Lyon-Caen, H., Armijo, R., Deschamps, A., Hatzfeld, D., Makropoulos, K., Papadimitriou, P., Kassaras, I., 1996. A microseismic study in the western part of the Gulf of Corinth (Greece): implications for largescale normal faulting mechanisms. Geophysical Journal International 126, 663–688.
Ring, U., Gessner, K., Gungor, T., Passchier, C.W., 1999. The Menderes massif of western Turkey and the Cycladic massif in the Aegean—do they really correlate? Journal of the Geological Society of London 156, 3–6.
Rutter, E.H., 1983. Pressure solution in nature, theory and experiments. Journal of the Geological Society of London 140, 725–740.
Saffer, D.M., Marone, C., 2003. Comparison of smectite and illite frictional properties: application to the updip limit of the seismogenic zone along subduction megathrusts. Earth and Planetary Science Letters 215, 219–235.
Schmidt, S.M., Handy, R.R., 1991. Towards a genetic classification of fault rocks: geological usage and tectonophysical implications. In: Muller, D.W., McKenzie, J.-A., Weissert, H. (Eds.), Controversies in Modern Geology: Evolution of Geological Theories in Sedimentology, Earth History and Tectonics. Academic, San Diego, Calif., pp. 339–361.
Scholz, C.H., 1998. Earthquakes and friction laws. Nature 391, 37–42.
Scholz, C.H., 2002. The Mechanics of Earthquakes and Faulting, 2nd edition. Cambridge University Press, p. 508.
Scognamiglio, L., Tinti, E., Michelini, A., Dreger, D.S., Cirella, A., Cocco, M., Mazza, S., Piatanesi, A., 2010. Fast determination of moment tensors and rupture history: what has been learned from the 6 April 2009 L'Aquila earthquake sequence. Seismological Research Letters 81, 892–906. doi:10.1785/gssrl.81.6.892.
Secor, D.T., 1965. Role of fluid pressure in jointing. American Journal of Science 263, 633–646.
Sibson, R.H., 1977. Fault rocks and fault mechanisms. Journal of the Geological Society of London 133, 191–213.
Sibson, R.H., 1985. A note on fault reactivation. Journal of Structural Geology 7, 751–754.
Sibson, R.H., 2000. Fluid involvement in normal faulting. Journal of Geodynamics 29, 469–499.
Smith, S.A.F., Faulkner, D.R., 2010. Laboratory measurements of the frictional strength of a natural low-angle normal fault. Journal of Geophysical Research 115, B02407. doi:10.1029/2008JB006274.
Smith, S.A.F., Holdsworth, R.E., Collettini, C., Imber, J., 2007. The role of footwall structures in the evolution of low-angle normal faults. Journal of the Geological Society 1187–1191.
Smith, S.A.F., Holdsworth, R.E., Collettini, C., 2011a. Interactions between low-angle normal faults and plutonism in the upper crust: insights from the Island of Elba, Italy. GSA Bulletin 123, 329–346. doi:10.1130/B30200.1 (January/February).
Smith, S.A.F., Holdsworth, R.E., Collettini, C., Pearce, M.A., 2011b. The microstructural character, evolution and mechanical significance of fault rocks associated with a continental low-angle normal fault: the Zuccale fault, Elba Island, Italy. (In Revision).
Spencer, J.E., 1984. The role of tectonic denudation in the warping and uplift of low-angle normal faults. Geology 12, 95–98. doi:10.1130/0091-7613(1984) 12.
Thatcher, W., Hill, D.P., 1991. Fault orientations in extensional and conjugate strike-slip environments and their implications. Geology 19, 1116–1120.
Townend, J., Zoback, M.D., 2000. How faulting keeps the crust strong. Geology 28, 399–402.

Walker, D.C., Anders, M.H., Christie-Blick, N., 2007. Kinematic evidence for downdip movement on the Mormon Peak detachment. Geology 35, 259–262. doi:10.1130/G23396A.1.
Wernicke, B., 1981. Low angle normal faults in the Basin and Range Province: Nappe tectonics in an extending orogene. Nature 291, 645–648.
Wernicke, B., 1995. Low-angle normal faults and seismicity: a review. Journal of Geophysical Research 100, 20159–20174.
Wernicke, B., Axen, G.J., 1988. On the role of isostasy in the evolution of normal fault systems. Geology 16, 848–851. doi:10.1130/0091-7613(1988) 016.
Westaway, R., 1999. The mechanical feasibility of low-angle normal faulting. Tectonophysics 308, 407–443.
Wright, L.A., Otton, J.K., Troxel, B.W., 1974. Turtleback surfaces of Death Valley viewed as phenomena of extensional tectonics. Geology 2, 53–54.
Yang, Z.H., Chen, W.P., 2008. Mozambique earthquake sequence of 2006: high-angle normal faulting in southern Africa. Journal of Geophysical Research 113, B12303. doi:10.1029/2007JB005419.
Yin, A., 1989. Origin of regional rooted low-angle normal faults: a mechanical model and its tectonic implications. Tectonics 469–482.
Zoback, M.D., et al., 1987. New evidence on the state of stress of the San Andreas fault system. Science 238, 1105–1111.
Zoback, M.D., Hickman, S., Ellsworth, W., 2010. Scientific drilling into the San Andreas fault. Eos 91 (22) (June 1).